

Aptamer-Based Detection of Caffeine and Theophylline Through
Utilization of Gold Nanoparticles and Graphene Oxide

by

Sarah Rebekah Labas

A thesis

presented to the University of Waterloo

in fulfillment of the

thesis requirement for the degree of

Master of Science

in

Chemistry

Waterloo, Ontario, Canada, 2023

© Sarah Rebekah Labas 2023

Author's declaration

I hereby declare that I am the sole author of this thesis. This is a true copy of the thesis, including any required final revisions, as accepted by my examiners.

I understand that my thesis may be made electronically available to the public.

Abstract

Both caffeine and theophylline are biologically important molecules, whose detection has become an area of interest. Because of their prevalence (caffeine consumption and theophylline in therapeutics) determining a quick, simple, and reliable way to detect these molecules has become a relevant problem.

With this in mind, two different biosensors were designed and tested. The first such sensor is an AuNP-based sensing method that was based on a previously reported mechanism. Unfortunately, previous reports failed to study and discuss how small molecule targets may be interacting with the AuNPs. With this, the goal of these experiments was to determine whether such an interaction existed and whether it affected the validity of the sensor. Using caffeine and its derivatives, we found that concentrations of caffeine and theophylline as low as $6.25\mu\text{M}$ were able to provide protection against salt-induced aggregation. As well, concentrations of derivatives, such as xanthine, were able to induce aggregation of AuNPs at concentrations as low as $5\mu\text{M}$. The results of these experiments confirmed that the interaction between AuNPs and target must be considered before using the mechanism as it has been previously reported; if such an interaction exists and is the dominant interaction in this sample, this sensing method cannot be used.

The GO-based sensor was designed by taking into consideration the fact that the adsorption of a fluorescently labelled aptamer onto GO will cause quenching of said fluorescent label. This sensor, when only GO and aptamer are present, is meant to have low fluorescence; once target has been added, it is intended that the aptamer preferentially interact with its target instead of GO. The dissociation of the aptamer from GO will result in an increase in

fluorescence, as the fluorophore will no longer be quenched. Studies using this method showed that although the method was successfully designed, as proven using a DNA and its cDNA as the probe and target, respectively, when assayed with the caffeine and theophylline aptamers, we found that the sensor was prone to nonspecific dissociation. Specifically, caffeine induced a greater fluorescence increase than theophylline when assayed with the aptamer specific to theophylline (3.27x the baseline for caffeine versus 2.9x for theophylline). To try to mitigate this, BSA was studied as a blocker, but was unsuccessful – it increased sensitivity while simultaneously decreasing selectivity of the sensor. Thus, the sensing method has the potential to be useful if an alternate blocking method is determined to be functional.

Acknowledgements

First and foremost, I would like to thank my thesis supervisor, Dr Juewen Liu, for providing me with endless support, and willingness to help whenever I needed it over the course of my degree. It was a pleasure to work with him as a mentor for these last two years. I would also like to thank Dr Vivek Maheshwari and Dr Mahla Poudineh, for agreeing to act as my committee members for this thesis. As well, I want to show my appreciation for some of the lab members, especially Dr Mohamad Zandieh, Dr Anand Lopez and Dr. Po-Jung Jimmy Huang, for their help with learning and understanding how to use equipment, and discussions about the concepts important to my work. Finally, I would like to thank some of the faculty who have been supportive of my time here during my undergraduate degree: Stacey Lavery, Dr Laura Marrone, and Dr Dara Gilbert. I would not have gotten to where I am today without you all.

Contents

Author's declaration	ii
Abstract.....	iii
Acknowledgements	v
List of Figures	viii
List of Abbreviations	ix
Chapter 1 - Introduction	1
Biosensors.....	1
Aptamers.....	2
Caffeine Aptamer.....	3
Theophylline Aptamer	5
Gold Nanoparticles	7
Aptamer-based biosensors	7
AuNP-aptamer based biosensors.....	8
Previously Proposed mechanism	9
Problems with mechanism	10
Graphene Oxide	11
Fluorescence	11
Sensing Mechanism	13
Target-Nanomaterial Interaction.....	14
AuNP-Target Interactions	14
GO-Target Interactions	15
Targets	16
Caffeine.....	16
Theophylline	17
Research Goals.....	18
Chapter 2 - Interactions Between Caffeine, Theophylline and Derivatives with Gold Nanoparticles and Implications for Aptamer-Based Label-Free Colorimetric Detection	20
Introduction	20
Results and Discussion	21
Colloidal stability of AuNPs in the presence of caffeine and related compounds.....	21
Protection of AuNPs by caffeine and theophylline indicative of adsorption.....	23

SERS to study adsorption	27
Protection of AuNPs by the aptamers.	28
Label-free colorimetric sensing of caffeine and theophylline	29
Conclusions	35
Experimental Section	36
Chemicals:	36
AuNP stability assays:	36
Aptamer-based sensing:	37
SERS and UV-vis Spectroscopy:	37
Chapter 3 - Graphene Oxide-Induced Quenching of Fluorescently Labelled Aptamers for Fluorescence-Based Detection of Caffeine and Theophylline	39
Introduction	39
Results and discussion	41
Effect of BSA.....	43
Verification of Method Design.....	45
Non-specific displacement.....	47
Concentration dependence	49
Target Effect on Fluorescence	51
Conclusions	52
Experimental section	53
Fluorescence analysis	53
Optimization of Sensor Conditions – Order of Addition	54
Polyethylene glycol (PEG)	54
Graphene oxide (GO) Optimization	55
Bovine Serum Albumin (BSA) optimization.....	56
References	58

List of Figures

Figure 1. Predicted structure of the Caff203 sequence.....	4
Figure 2. Predicted structure of the Theo2201 aptamer.....	6
Figure 3. The structures of caffeine and derivatives.....	23
Figure 4. Stability assays of AuNPs with caffeine and its derivatives.....	24
Figure 5. pH dependence of protection effect offered by theophylline.....	25
Figure 6. Protection of AuNPs offered by caffeine and theophylline and SERS results.....	28
Figure 7. Protection against aggregation offered by caffeine and theophylline aptamers.....	29
Figure 8. Sensing mechanism and data summary.....	30
Figure 9. Assays using alternate NaCl concentrations.....	32
Figure 10. Paraxanthine-induced AuNP colour change kinetics.....	33
Figure 11. Possible results for the sensing assay when the target is dominating the system.....	34
Figure 12. Nonspecific dissociation of 002 sequence by caffeine and theophylline.....	43
Figure 13. Fluorescence enhancement with and without BSA (caffeine aptamer).....	44
Figure 14. Fluorescence enhancement with and without BSA (theophylline aptamer).....	45
Figure 15. Specific and nonspecific dissociation of the FAM 24-mer sequence.....	46
Figure 16. Structures of each of our small molecule targets.....	47
Figure 17. Adenosine as a nonspecific target.....	48
Figure 18. Specific and nonspecific dissociation of the FAM adenosine aptamer.....	48
Figure 19. Concentration dependence of caffeine aptamer.....	50
Figure 20. Concentration dependence of theophylline aptamer.....	50
Figure 21. Direct effect of targets on fluorescence.....	51

List of Abbreviations

DNA – Deoxyribonucleic Acid

RNA – Ribonucleic Acid

SELEX – Systemic Evolution of Ligands by Exponential Enrichment

PCR – Polymerase Chain Reaction

HEPES – 4-(2-hydroxyethyl)-1-piperazineethanesulfonic acid

ITC – Isothermal Titration Calorimetry

Caff – Caffeine

Theo – Theophylline

UV Vis – Ultraviolet Visible

NaCl – Sodium Chloride

AuNP(s) – Gold nanoparticle(s)

cDNA – Complimentary Deoxyribonucleic Acid

FRET – Fluorescence Resonance Energy Transfer

FAM – Fluorescein Amidite

GO – Graphene Oxide

As^{III} – Arsenic(III)

COPD – Chronic Obstructive Pulmonary Disease

RFU – Relative Fluorescence Units

BSA – Bovine Serum Albumin

PEG₂₀₀ – Polyethylene Glycol (200 unit repeats)

Chapter 1 - Introduction

Biosensors

Biosensors “are devices which combine a biological component to detect an analyte and a physicochemical component to produce a signal which is measurable”.¹ According to this definition, in a biosensor that couples aptamers with nanomaterials, the aptamer acts as the biological component, which serves to detect the target of interest, and the nanomaterials act as the physicochemical component, which serves to produce a signal that is measurable.

Aptamers are an excellent choice as the biological component of a biosensor because there already exists a wide array of aptamer sequences, which can bind tightly and specifically to a variety of targets.^{2,3} Additionally, the selection of new aptamer sequences for binding new targets is relatively straightforward. The selectivity of aptamers is desirable, as it reduces the likelihood of a false-positive result from any alternate targets that may come into contact with the sensor. Additionally, if a sample being assayed is not pure, but the detector portion of the sensor is specific to a singular target, this has the potential help reduce the likelihood of a false result from contaminants in a sample.^{2,3}

Sensitivity of the biosensor is another important quality; the more sensitive a sensor is, the lower the limit of detection for its target. This is something that would be especially important in sensor applications like water remediation, for detecting contamination, or in pharmaceuticals, for detecting a given target in a patient-provided sample.^{2,3}

The nanomaterial used in the sensor will serve as the signal transduction portion of the biosensor. For example, in a gold nanoparticle-based sensor, there will be a visual colour

change, which can be directly correlated to a change in the absorbance spectrum of a sample.⁴⁻⁷ Similarly, graphene oxide acts as a fluorescence quencher; when target is present, the fluorescence signal is meant to increase, in a way that is proportional to the concentration of the target.⁸ This signal change is easily measured using fluorometry. In both cases, the nanomaterials have chemical properties which allow them to, when partnered with an aptamer and a target, produce a change that is measurable and directly proportional to the concentration of said target.

Together, aptamers and nanomaterials possess the qualities needed to create a biosensor. These works will focus on the design and testing of biosensors that are made with a combination of aptamer and nanomaterial. These types of designs are favourable, as once they are appropriately optimized, they are generally simple to produce and execute for reliable detection of a single target.

Aptamers

An aptamer is a short, single-stranded DNA or RNA sequence that is used to bind tightly and specifically to a given target. Aptamers have been shown to bind specifically to proteins, small molecules, peptides, carbohydrates, toxins, or even whole, live cells.^{2,9} Generally, aptamers are selected using a process called systemic evolution of ligands by exponential enrichment, or SELEX. The SELEX process consists of three major steps : 1) incubation of target molecules with a pool and random sequence single stranded DNA molecules; 2) separation of free (unbound) sequences from sequences that are bound to targets; and 3) amplification of

bound aptamers using PCR. The process continues for many rounds, with increasingly stringent conditions, to obtain only the sequences with the highest affinity and specificity.^{2, 10, 11}

Caffeine Aptamer

Due its near-ubiquitous consumption, there was an interest in selecting an aptamer that was highly specific for caffeine, that is able to distinguish between caffeine and its derivatives, namely theophylline, theobromine, and xanthine.¹² The selection of such an aptamer was done by Huang and Liu.¹⁰ Their selection was based on previous SELEX methods detailed by Yang, but was performed using some modifications.^{13,14} The first step of their selection was to anneal the library with a 5-fold excess of biotinylated capture strand, along with a SELEX buffer. The purpose of this high salt buffer (500mM NaCl, 10mM MgCl₂, and 50mM HEPES, pH 7.5), was to screen any nonspecific electrostatic interactions that may be occurring during the annealing process.¹⁰

Once annealed, the DNA was then run through a streptavidin agarose resin-packed micro chromatography column several times. The column was then washed 12 times over, using the SELEX buffer, to remove any unbound or loosely bound sequences. Following the wash, a caffeine solution was then passed through the column; any sequences that eluted during this step were then collected and amplified using PCR. Next, a biotinylated reverse primer was used to obtain the PCR products, which were then concentrated and further purified for sequence analysis. A total of 20 rounds of selection were done, with counter selection for the caffeine analogue, theophylline, starting at round 13 of the selection. After 20

rounds of selection, some sequence convergence became evident, with the converged sequence being present in 29% of the final library selected.¹⁰

To assess the binding potential of the selected aptamers, isothermal titration calorimetry (ITC) was used. These results showed that for all sequences selected, there was the highest affinity for caffeine, suggesting a successful selection process. The Caff203 sequence presented the strongest binding affinity to caffeine, giving a dissociation constant, K_d of $2.2\mu\text{M}$, and showed little to no binding to the analogue targets that were tested. The Caff203 sequence selected as described was used in experiments presented and discussed in this thesis. The predicted structure of this aptamer is shown in Figure 1. The region highlighted in red shows the convergent region, which began to emerge after 20 rounds of selection. The sequence of the Caff203 aptamer is 5' GAC GAC TAC GGA GTT TTA GCC GTC ACG TTC CCA GGA GTC GTC 3'.¹⁰



Figure 1. Predicted structure of the Caff203 sequence, as selected by Huang and Liu.¹⁰

Theophylline Aptamer

In 1994, Jenison *et al.* reported the selection of an RNA aptamer for theophylline, which showed a 10,900-fold affinity for theophylline over caffeine, despite the minute difference in structure, of only a single methyl group.^{11,15} This aptamer has since been used for a variety of applications, such as RNA switches, biosensors for theophylline, and riboswitches.¹¹ Despite its incredibly high selectivity, the usage of RNA aptamers is less favourable compared to DNA aptamers, since DNA aptamers are both less expensive to produce and are much more stable molecules.¹¹ Because of this, Huang set out to select a new theophylline aptamer, that was instead made from DNA.

To isolate the aptamer, library immobilization was used. The DNA library used for the selection contained a random region, 30 nucleotides in length. The library was designed with the intention of folding into a hairpin structure once bound to theophylline. With this in mind, the library was immobilized using hybridization onto a streptavidin column – the expectation was that any sequences that were able to bind theophylline would form into the aforementioned hairpin structure, thus freeing them from the column. Any strands that were liberated were then amplified using PCR and used in further rounds of selection.¹¹

After 11 rounds of selection, counter selection using caffeine was performed, to increase the selectivity of the aptamer to theophylline. Of the sequences selected, there were 20 that showed 19 nucleotides that were highly conserved; some sequences had the nucleotides in reverse, though the bases were still conserved.¹¹ These results suggest a successful selection of the aptamer.

Binding assays to determine the detection limit and the selectivity of the aptamer were done using ITC. This method serves to measure the heat of binding and can be done using label-free aptamers. These experiments gave a dissociation constant, K_d of $0.51 \pm 0.13 \mu\text{M}$. When analogs of theophylline, namely caffeine, theobromine and paraxanthine, were assayed, none of these targets showed a heat change – i.e., no binding was observed.

For the experiments discussed in this thesis, the Theo2201 sequence from this selection was used. The sequence of this aptamer is: 5' GAC GAC GAT TGT GGT CTA TTC ATA GGC GTC CGC TGA GTC GTC 3'. The predicted structure of the aptamer, with the highly conserved region shown in red, green, and blue is shown in Figure 2.

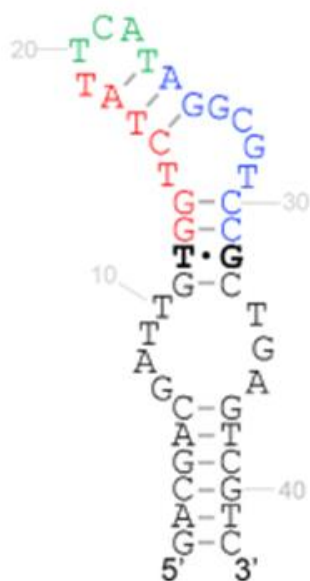


Figure 2. Predicted structure of the Theo2201 aptamer, as selected by Huang and Liu.¹¹

Gold Nanoparticles

Aptamer-based biosensors

Aptamers, both RNA and DNA have been incredibly attractive components for a variety of applications for quite some time.^{2,9,16} Aptamers can be used for the design of biosensors for an array of applications, such as detection of contaminants for environmental monitoring, or biomedical diagnostics.^{17,18} Aptamers are so widely used and desirable because of their ability to bind to a given target with a great degree of specificity, and generally have very good sensitivity. Aptamers can be used in biosensors that are labelled, for example with a fluorophore, for analysis using fluorometry, or unlabelled, if another component of the biosensor is able to transmit a signal.^{1,3,18} Aptamers are also useful for a variety of analysis methods, depending on your target and desired sensor conditions. Some instrumentation that can be used for these types of analyses include fluorometry, upconverting nanoparticles, magnetic resonance imaging, flow cytometry, nanoflare technology, electronic aptamer-based sensors, or lateral flow devices.^{17,18}

Despite their desirable qualities, there exist some limitations to using aptamers for biosensing applications.^{2,18} Although aptamers can be selected at high specificity and affinity, the process of selection of an aptamer can be quite lengthy. Additionally, there is a finite number of sequences that can be generated, and not all sequences will be viable for usage as an aptamer. As well, despite their high specificity, aptamers are optimally used in pure samples with minimal contamination. Contamination in samples may affect the reliability and accuracy of analysis with an aptamer-based sensor, which limits their practical usage.¹⁸

AuNP-aptamer based biosensors

Gold nanoparticles are attractive for usage in an aptamer-based biosensor because they provide both qualitative sensing data – a colour change visible without equipment – and quantitative data, wherein this visual colour change can be tracked using UV-Vis spectrometry.⁴⁻

⁷ The first iteration of the mechanism for AuNP-based sensing using label-free aptamers worked using double stranded DNA; in this mechanism, the target DNA was the complimentary sequence to the probe DNA.^{19,20} Because double stranded DNA cannot interact with the surface of gold nanoparticles, as the nucleobases are preferentially interacting with the complimentary strand nucleobase, the resulting colour change, or lack thereof, was clearly indicative of presence vs absence of target.^{19,20}

To track the changes in a quantifiable way, UV Vis spectroscopy is used for this type of biosensing method. When AuNPs are freely dispersed, they appear a deep red colour, and have a maximum absorbance of approximately 523nm.^{21,22} Once AuNPs have been aggregated, a change which is irreversible, they become a blue or purple colour, and absorb maximally over a wider wavelength range, approximately 600-700nm. To determine whether a sample contains more freely dispersed or more aggregated nanoparticles, the ratio of absorbances at these wavelengths was calculated. Specifically, the absorbance is given as the ratio as follows: $\left(\frac{Abs_{620}}{Abs_{523}}\right)$.

In this way, a small ratio is indicative of freely dispersed AuNPs, as the absorbance at 523 is higher, whereas a larger absorbance ratio is indicative of aggregated nanoparticles, given that the absorbance at 620nm is higher.^{21,22} Fully aggregated nanoparticles by way of adding NaCl give an absorbance ratio around 1.

The clear and relatively quick colour change seen with salt-induced aggregation of AuNPs makes their usage in a biosensor a favourable method for detection. The visible colour change of AuNPs eliminates the need to label the aptamer that is used in tandem. Labelling aptamers can be both expensive and time consuming, since studies must be done to determine which type of label is best, what kind of instrumentation is needed for analysing a certain label, among other factors that must be optimized.^{2,5} Thus, eliminating the need for a label with this method is highly sought after in research geared towards designing biosensors. Additionally, UV Vis spectroscopy is a quick way to obtain results, which, again, makes for the favourable design for a biosensor, as results can be obtained relatively quickly. This method of analysis also provides reliable results.

Previously Proposed mechanism

There exists a previously reported aptamer-based label-free biosensor that uses gold nanoparticles for the detection of small molecules. This method originally was designed using a DNA probe, with complimentary DNA as the target.^{19,20} This method by design worked by utilizing the protection effect offered by single stranded DNA. Specifically, AuNPs are susceptible to aggregation when mixed with salt; when AuNPs become aggregated, they transition from a red colour (freely dispersed) to a blue or purple colour (aggregated). In this case, NaCl was the salt that was used. However, single stranded DNA can interact with the surface of AuNPs in a way that provides protection for the AuNPs against salt-induced aggregation. Additionally, double stranded DNA cannot protect against salt-induced aggregation. Using this knowledge, a sensor was designed, wherein the probe DNA was first

allowed to interact with the AuNPs to act as a shield against aggregation. Next, NaCl was added to the mix; because DNA is protecting against aggregation, no colour change will occur. Finally, the target DNA (the cDNA strand that is complimentary to the probe) is added.^{19,20}

In this mechanism, once the target DNA has been added, the probe DNA will preferentially interact with the cDNA as opposed to the AuNP surface.^{19,20} When this occurs, the protection effect offered by DNA decreases as less DNA interacts with AuNPs – this causes the aggregation of AuNPs as NaCl is able to interact with the now exposed AuNPs. If no cDNA is added or if an alternative non-specific target is added, the proposed mechanism suggests that the protection effect will remain, since the probe DNA is specific only to its cDNA target. Thus, no aggregation, and no colour change, will occur.^{19,20}

The method as designed is dependent on the idea that: single stranded DNA can protect against salt-induced aggregation, double stranded DNA cannot, NaCl is the only component of the sensor that can induce aggregation, and that the single stranded probe DNA is the only component that can protect against salt induced aggregation.

Problems with mechanism

Although the initial design of this sensing mechanism is elegant in its simplicity, a very important part for success of this mechanism exists in the fact that single stranded DNA can, and does, interact with the surface of the AuNPs, whereas double stranded DNA cannot. Later works used this mechanism as a method to detect small molecules, such as arsenic or adenosine, and were also used to prove that an aptamer sequence was successfully selected for a given target.²³⁻²⁵ These experiments, however, failed to take into consideration the

interaction between the small molecule target and the AuNPs.^{24,25} This could lead to false positive and false negative results and may also lead to incorrect conclusions as to the cause of the colour change.

The extension of the method for the detection of small molecules introduces the targets themselves as an additional variable, which did not need to be considered when the target of the mechanism was also single stranded DNA. However, when small molecules were used as the target for this sensing mechanism, the potential interaction between the target and AuNPs was not considered.^{24,25} Although we know for sure double stranded DNA will not interfere with the sensing mechanism, we cannot guarantee that the targets being used will not do so either.²⁶ In particular, there exists the possibility that the target can interact with the AuNPs in a way that is either stabilizing – which may prevent a salt induced colour change, or, the target may induce a colour change itself, both of which are unintended and unwanted interactions.

Because the target-gold interaction has yet to be considered in previous uses of this sensing mechanism, a goal of the work presented in this thesis was to determine whether such an interaction existed, and, if so, whether said interaction interferes with the sensing mechanism in a way that renders the mechanism inviable.

Graphene Oxide

Fluorescence

The first instance of fluorescence being observed occurred in 1656, which was detailed in an excerpt of Monardes' *Ligirium mephiticium*; since this observation, fluorescence has continued to be studied by a number of scientists.²⁷ Fluorescence and fluorescent labels have

been studied so intently, because of their breadth of applications – particularly in the field of molecular biology and its subfields, for the purpose of live cell imaging, protein structure and function analysis, as well as localization of cellular components.²⁸ Fluorescent labels are also the most commonly used method for the purpose of biosensing, because of the diversity in labels available, because they are simple to use, and because they are quite sensitive.²⁸

Fluorescent labels are also very appealing in the field of nanotechnology and nanomaterials, as will be presented in these works. These types of labels are being favoured over typical organic dyes, because of their superior optical properties.²⁹ Fluorescent labels offer a brighter fluorescence, greater degrees of photostability, better sensitivity, and a wider range of emission and excitation wavelengths compared to their organic dye counterparts.

Additionally, these labels can be used for a variety of sensing assays, including, but not limited to, basic fluorescence assays, fluorescence resonance energy transfer (FRET), fluorescence lifetime measurement, and multiphoton microscopy. Each of these sensing techniques can be used in tandem with nanomaterials.²⁹

Fluorescence works as a transfer of energy. In simple terms, molecules that fluoresce do so by absorbing photons of specific wavelengths, and subsequently emitting these same photons at slightly higher wavelengths.²⁸ Light can act as an electromagnetic field – it can induce oscillations by way of resonance – to the electrons of a fluorophore. This interaction can cause a single paired electron to be ejected from its stable ground-state orbital into a higher-energy excited-state orbital. The fluorophore's ability to absorb photons at specific wavelengths is correlated to amount of energy required to push an electron from a ground state to an

excited state. The state of excitation lasts only for a very limited amount of time, with vibrational relaxation occurring between high energy excited states, resulting in a loss of energy. The loss of energy causes the electron to fall back into the stable ground-state orbital; this energy is most often released as a photon, though can also be released as a loss of heat or from other processes. The photon that is emitted is done so with lower energy than the photon that was absorbed – this is the emission wavelength. It is the absorption and emission of photons that gives fluorophores their fluorescence.²⁸

In the experiments described in this thesis, the fluorescence label fluorescein amidite, or FAM, was used. This fluorescent label is the most commonly used fluorescent dye for labelling oligonucleotides, like aptamers. FAM has a maximum absorbance wavelength of 492nm, and a maximum emission wavelength of 517nm.²⁷

Sensing Mechanism

Graphene oxide is known to be able to interact with single stranded DNA sequences, like aptamers. Nucleobases, when exposed, form an electrostatic interaction with the surface of graphene oxide – i.e., DNA can adsorb onto the graphene oxide surface.³⁰⁻³² This interaction persists when an aptamer is fluorescently labelled. When a fluorescently labelled aptamer adsorbs onto GO, the result is the quenching of the fluorophore. Although the specific mechanism that causes the quenching has not been formally studied, a potential explanation may be that adsorption alters the structure of the aptamer in a way that prevents the fluorophore from fluorescing.³⁰⁻³²

Considering this interaction, another relatively simple biosensing method can be designed. When a fluorescently labelled aptamer is freely dispersed in solution, we have fluorescence. Once GO is added, the aptamer will adsorb on the surface of the graphene oxide lattice, which results in the quenching, or reduction, of the fluorescence output of the fluorophore. When the target of the aptamer is added, it is predicted that the aptamer will preferentially interact with its target, releasing it from the GO surface, resulting in an increase in the fluorescence output – we get enhancement. With this, when we see fluorescence enhancement, it is meant to demonstrate the presence of the target and confirm binding. If no fluorescence enhancement is observed, it is meant to indicate a lack of binding.³⁰⁻³²

Target-Nanomaterial Interaction

AuNP-Target Interactions

Previous iterations of the AuNP aptamer-based sensing mechanism have been used to prove the binding of newly selected aptamers to their targets.^{23,33} An example of the described mechanism being used to this end is in experiments done to demonstrate the selection and proof of binding of an arsenic aptamer to As^{III}.²³ In these works, authors describe the AuNP-based biosensor that they have used for proving that their newly selected aptamer is able to bind to its intended target, arsenic.²³ However, what authors failed to study or discuss was the interaction between AuNPs and arsenic(III) itself; reported results only discuss the final outcome of the sensing experiments, which were interpreted as successful binding of aptamer to target.

This work was later discussed in an article by Zong *et al*, where authors perform alternate binding assays, such as spectroscopy experiments and ITC to study the binding of arsenic(III) to its reported aptamer.²⁴ Here they find that As^{III} has a notable interaction with AuNPs, and are able to adsorb onto the surface of AuNPs. As well, this interaction is strong enough to displace DNA that has been adsorbed onto AuNPs already, and can prevent adsorption of DNA if As(III) has already been adsorbed.²⁴

With these findings in mind, it is important to study the interaction between AuNPs any molecule that is intended to be used as the target for the AuNP aptamer-based detection method. Although Zong reports that an interaction between As(III) and AuNPs exists, the effect that this interaction may have on the sensing method was not directly studied. Consequently, the works described in this thesis were done with the goal of assessing how any potential interaction between AuNPs and target may affect the sensing method as reported.

GO-Target Interactions

Graphene oxide exists in single layer 2-dimensional lattices, as sp^2 -hybridized carbons.³⁴ The structure of graphene oxide lends itself to a number of favourable physical-chemical properties, such as a high fracture strength, exceptional thermal and chemical conductivity, a high Young's modulus, large specific surface area, as well as biocompatibility. These qualities are what contribute to GO being an appealing nanomaterial for usage in a variety of applications, such as in biosensors, as nanocarriers for drug delivery, in biological imaging or as probes for cells.³⁴

Graphene oxide has been shown to interact with single stranded DNA, as the DNA bases can form electrostatic interactions with the surface of the GO lattices through the lone pairs on their nitrogenous bases.^{8,34} Despite this, however, literature searches showed that not much work has been done to assess how non-DNA targets may be interacting with the GO lattices. Though not the central focus of the work presented in this thesis, the interaction between graphene oxide and targets, and the effect that this interaction may have pertaining to biosensing applications, is discussed.

Targets

Caffeine

Caffeine is the most commonly and widely consumed psychoactive substance worldwide, though especially in North America.¹² Because of its prevalence in the human diet, the potential for negative environmental impacts has become of increasing interest.^{10,35-38} Although studies have shown that caffeine has negative affects only in a small subset of individuals, the potential for harm to coastal ecosystems and plant life is relatively high.³⁵ Because of this, it is important to be able to detect caffeine quickly and reliably, to monitor when concentrations may be reaching a hazardous point in susceptible environments. Easy and quick detection can allow for quicker transitions to remediation efforts when needed.

Caffeine has four methyl groups; when any one of these methyl groups is removed, the structure represents one of a few derivatives of caffeine – theophylline, paraxanthine, theobromine or xanthine. Studying how these derivatives may affect the efficacy of a caffeine sensor is important to determine how specific a given sensor is to caffeine, and how well it can

distinguish caffeine from its derivatives. In the AuNP based sensor discussed in this thesis, the ability of the sensor to differentiate between these derivatives is studied.

Theophylline

Theophylline is the caffeine derivative that results from the demethylation of carbon 7 on caffeine (Figure 3). In the past, theophylline had been used to treat patients who suffer from asthma and chronic obstructive pulmonary disease (COPD), by acting as a bronchodilator.^{39,40} In more recent years, however, its usage has been more geared towards treating bradycardia and apneas in premature newborns in the United States. Despite its applications in therapeutics, the actual therapeutic window of theophylline is quite narrow; even small overdoses above the therapeutic range can result in both acute and chronic adverse affects.^{39,40}

Theophylline's therapeutic effects are a result of an indirect stimulation of β -1 and β -2 receptors, which causes the release of catecholamines, which, in low concentrations, can allow proper bronchodilation. When theophylline concentrations reach above the (narrow) therapeutic concentration range, the release of excess catecholamines can cause issues relating to cardiovascular, neurological, metabolic, musculoskeletal, and gastrointestinal systems; the severity of the toxicity of theophylline is related to the dosage and route of exposure.^{39,40}

Because of its usage in therapeutics, and the potential for very dangerous overdoses if improperly dosed or administered, monitoring of theophylline levels is an important and relevant issue for medical practices. Detecting concentrations of theophylline quickly and

reliably may be able to aid in decreasing the occurrences of theophylline overdoses, by facilitating its monitoring, to assess when levels may be approaching the threshold for toxicity.

In addition to the toxicity related to the overdosage of theophylline in therapeutics, because theophylline is used in pharmaceuticals, there also exists the possibility of environmental contamination, from runoffs originating from wastewater treatment plants.⁴¹ The existence of theophylline in the environment can also have adverse affects, once again indicating the importance of its reliable detection and quantification.⁴¹

Research Goals

Given the information provided here, the research presented in this thesis was performed to determine whether an interaction between target and AuNPs existed. Once an interaction was assessed, it was investigated whether said interaction would affect the validity of previous reports of an aptamer-based label-free colorimetric detection mechanism using AuNPs. Experiments were done to study the protection afforded by the chosen aptamers, the destabilization effect of NaCl on AuNPs, the interaction of specific and non-specific targets with AuNPs, and the effect of each of these interactions on the previously proposed sensing mechanism.

Following the investigation of a target-gold interaction, another possible sensing mechanism, using graphene oxide, was then designed, and studied, as an alternate way to detect caffeine and theophylline. This method used fluorescently labelled (FAM) aptamers for a fluorescence-based detection mechanism. Specific and nonspecific dissociation, the effect of

blocking, and concentration dependence were investigated using each the caffeine and theophylline aptamers. The sensor was also assayed using a few alternative DNA sequences and targets to further assess the validity and success of the method as designed.

Chapter 2 - Interactions Between Caffeine, Theophylline and Derivatives with Gold Nanoparticles and Implications for Aptamer-Based Label-Free Colorimetric Detection

Introduction

Caffeine is a very important molecule due to its widespread consumption.¹² It is extensively and readily available and is the most widely used psychoactive substance. The widespread consumption of caffeine has caused concentrations to rise in the environment and aquatic ecosystems. Although negative effects on humans have not been a major concern, there are reports of possible negative effects on coastal ecosystems.³⁵ For physiological and environmental reasons, its detection and quantification are an area of growing interest.^{10,36-38}

The chemical name of caffeine is 1, 3, 7-trimethylxanthine, where removing any of the methyl groups generates three new molecules named theophylline, theobromine and paraxanthine, respectively. Theophylline is a main active component in tea, and it has been used to treat airway diseases such as asthma.⁴⁰ A lot of efforts have been made pertaining to the detection and quantification of theophylline, especially in blood, due to its pharmaceutical relevance.^{40,42,43}

Our lab recently reported a series of DNA aptamers that can bind caffeine¹⁰ and theophylline,¹¹ respectively. These aptamers can be used to develop biosensors for selective detection of these molecules. Gold nanoparticles (AuNPs) have been very popular in developing aptamer-based biosensors because of their excellent optical properties.^{4-7,17,44-45} Many sensors were designed by taking advantage of the protective effect of aptamers against salt-induced

aggregation of AuNPs.¹⁹⁻²⁰ Aptamer binding to its target was also believed to inhibit aptamer adsorption to AuNPs, and thus AuNPs are easily aggregated upon adding salt.⁴⁶⁻⁴⁹ The color change due to AuNP aggregation can thus indicate the presence of target analytes. This method hinges on the idea that of the components in the sensor, only DNA aptamers can provide stability against salt induced AuNP aggregation, and only salt can induce aggregation.

However, we recently discovered that the adsorption of many target analytes to AuNPs needs to be considered.⁵⁰ Ignoring such an interaction has led to false positives (seeing aptamer binding where none exists) if aggregation is induced by the target.^{26,51} False negatives are also possible, wherein no aggregation is occurring regardless of whether the aptamer is binding to the target, because excess target is protecting AuNPs against salt-induced aggregation.^{21,52}

The adsorption of caffeine, theophylline and other methylxanthines on silver nanoparticles was studied in previous works, though the adsorption of these molecules on AuNPs has yet to be reported.⁵³⁻⁵⁵ We herein systematically studied the adsorption of caffeine, theophylline, and related compounds to gain fundamental insights. We also tested the AuNP-based detection method and concluded that this method cannot be directly used for the detection of caffeine or theophylline due to the adsorption of these molecules onto AuNPs.

Results and Discussion

Colloidal stability of AuNPs in the presence of caffeine and related compounds.

The structures of caffeine and related compounds tested in this work are shown in Figure 3. Each of these structures consists of the same xanthine core with different numbers of methyl groups. Freely dispersed AuNPs are red in colour. When they become aggregated, their

visual appearance shifts to a purple or blue color. For the as-synthesized citrate-capped AuNPs, and the AuNPs with added caffeine, theophylline, and theobromine, we saw an identical red colour, indicating that these molecules did not induce aggregation (Figure 3). This differs from the purple and blue color that resulted upon the addition of paraxanthine and xanthine, respectively, which are indicative of aggregation of our AuNPs.

This color change also shifted the wavelength at which maximum absorbance is observed. Freely dispersed AuNPs absorb maximally around 520–525 nm, and aggregated AuNPs absorb over a wider range, around 600–700 nm. To quantify the color, UV-vis spectroscopy was used, and absorbance ratios (620 nm/523 nm) were determined. Given that aggregated AuNPs absorb higher at 620, and freely dispersed AuNPs absorb more at 523, high absorbance ratios indicate that the AuNPs are aggregated, and low ratios are indicative of freely dispersed AuNPs.

Since adenosine-induced aggregation of AuNPs has been well studied,²¹⁻²² we also included adenosine and adenine in this experiment for comparison. Adenosine-induced aggregation is evidenced by the increasing ratio of absorbance as the concentration of adenosine increases, with aggregation starting at very low concentrations (Figure 4A). The fitting shown in Figure 4A for adenosine resulted in an apparent K_d of adenosine to AuNPs of 7.2 μ M. To contrast this, as the concentrations of both caffeine and theophylline were increased to even 500 μ M, the ratio of absorbance remained low and comparable to that of the pure AuNPs, which is indicative of a lack of aggregation.

In contrast, xanthine and paraxanthine showed increasing ratios of absorbance as the concentrations of these targets increased (Figure 4B). Both targets can readily induce aggregation starting at low micromolar concentrations and reach a plateau at approximately 5 μ M. Theobromine is comparable to caffeine and theophylline in that increasing the concentration has no significant effect on the absorbance ratio, suggesting that theobromine cannot induce aggregation.

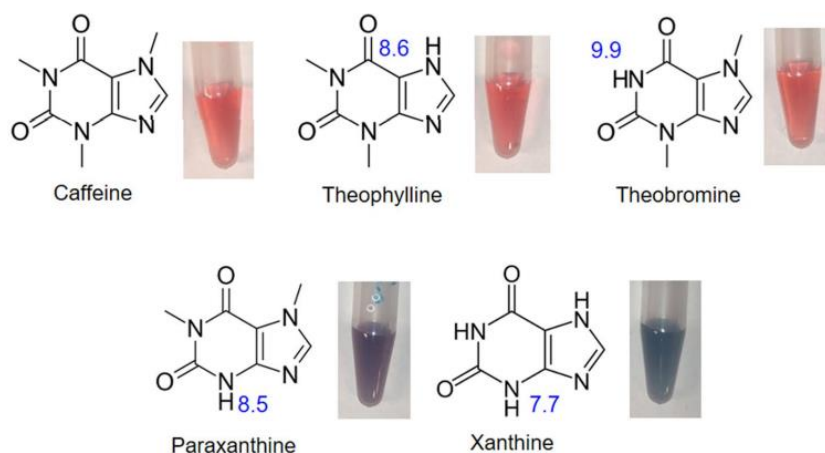


Figure 3. The structure of caffeine and its derivatives, and photographs of AuNPs following the addition of caffeine, theophylline, theobromine, paraxanthine and xanthine, respectively. Samples have final concentrations of 4.6nM AuNPs, 2.5mM MES buffer, pH 6.1 and 500 μ M target. pKa values are shown in blue, next to the proton that they correspond to. All pKa values given were taken from their respective PubChem compound summary sheets.⁵⁶

Protection of AuNPs by caffeine and theophylline indicative of adsorption.

Given that no target-induced aggregation was observed for either caffeine or theophylline, it was unclear whether these two molecules can be adsorbed to AuNPs. To test this, we then determined whether these two molecules would protect AuNPs against salt-

induced aggregation. To ensure that any protection observed can be afforded to the presence of the target of interest, no buffer was included in these methods. Samples were prepared using AuNPs, target and NaCl exclusively. For both caffeine and theophylline, increasing their concentration decreased the absorbance ratios (Figure 6A). Thus, we can conclude that they protected AuNPs against salt-induced aggregation.

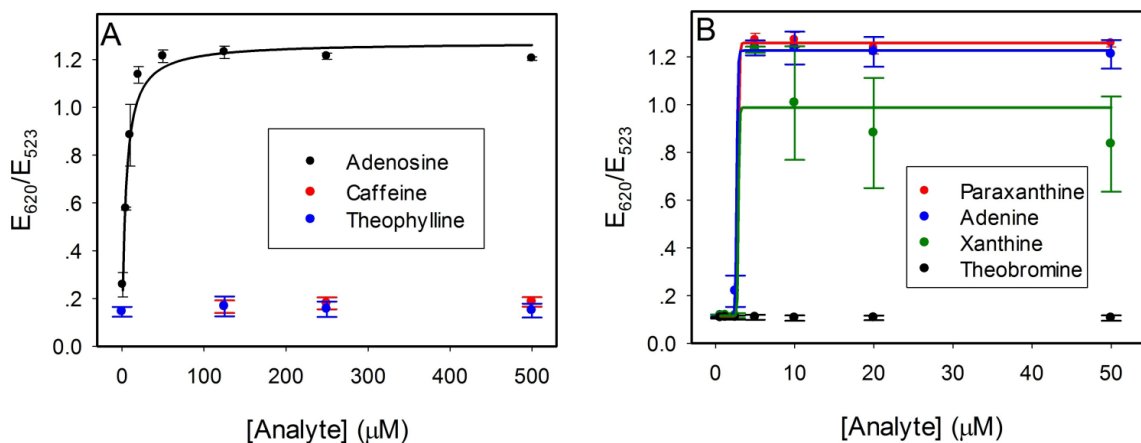


Figure 4. (A) The extinction ratio of the AuNPs in the presence of caffeine, theophylline, and adenosine. Adenosine was included as a positive control. **(B)** The extinction ratio of the AuNPs in the presence of paraxanthine, theobromine, xanthine, and adenine. Experiments were repeated in triplicate.

Protection plateaus at approximately $125\mu\text{M}$ for both caffeine and theophylline, with noticeable protection being observed starting at $6.3\mu\text{M}$ for both studied targets. Such protection was indicative of adsorption of these two molecules to AuNPs. The effect of pH on the protection afforded by theophylline was also studied. Both acidic (pH 4.2) and basic (pH 10.2) conditions were assayed. These experiments showed an increase in protection at low concentrations of theophylline at pH 10.2, and a slight decrease in protection at the lowest

concentrations of theophylline at pH 4.2 (Figure 5). Protection remained comparable at concentrations greater than $6.3\mu\text{M}$ for each reaction condition. These results indicated that pH does not have a notable impact on the protection offered by theophylline. The NaCl control (no theophylline) at pH 10.2 also had a slightly decreased ratio of absorbance. Thus, the pH 10.2 buffer itself may be contributing to the slight increase in protection shown in Figure 5.

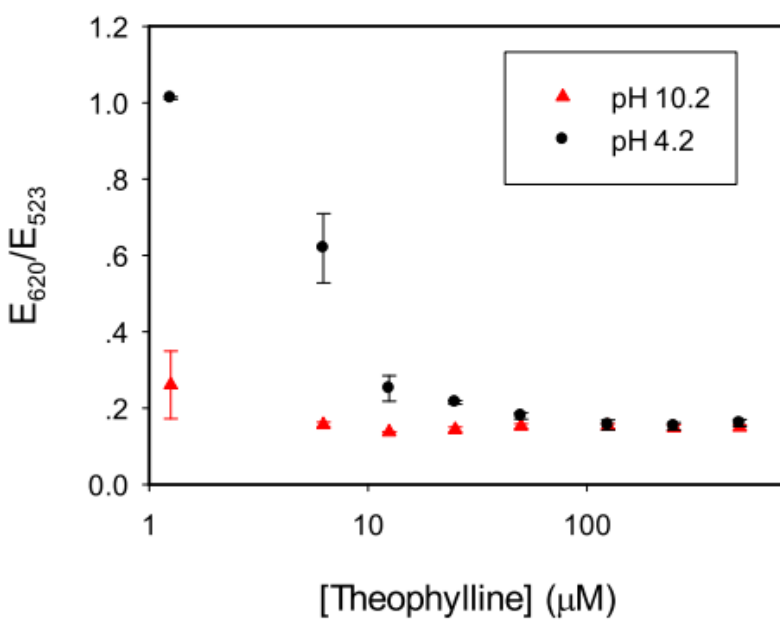


Figure 5. pH-dependent studies to assess whether the pH of the samples affected the protection afforded by theophylline. An acidic pH (4.2) and a basic pH (10.2) were studied. Compared to the unbuffered samples (Figure 6), when theophylline concentrations were $<10\mu\text{M}$, the pH 10.2 samples showed increased protection, and the pH 4.2 samples showed slightly decreased protection. When the concentration of theophylline was greater than $6.3\mu\text{M}$, protection was comparable for all three samples. These results indicate that pH did not have a significant impact on the protection against salt-induced aggregation afforded by theophylline.

When comparing the structures of caffeine and its derivatives (Figure 3), there is a notable difference between the compounds that can induce aggregation and those that do not. It is tied to the presence versus absence of a methyl-capped nitrogen in the N3 position. The N3 methyl-cap is missing on xanthine and paraxanthine and these are the only caffeine derivatives studied here that induced aggregation. Caffeine, theophylline, and theobromine are methyl-capped on this nitrogen, and none of these compounds induced aggregation of the AuNPs. Given this, we reasoned that the structures of the targets being studied are critical in determining whether an interaction would stabilize or destabilize AuNPs. Note that they were all adsorbed to the AuNPs.

The charge of a molecule is known to strongly influence its ability to stabilize AuNPs. For example, adenosine destabilizes AuNPs, while ATP stabilizes them, since the latter has a negatively charged triphosphate.²¹ At our experimental condition pH of 7.3, each of these molecules exists in a neutral charge state (0 formal charge). With this, the pKa values of these molecules (shown in Figure 3) do not seem to be an important parameter for determining whether a target may have a stabilizing or destabilizing effect on AuNPs.

A possible explanation for the lack of methyl cap contributing to aggregation is that this N3 position can coordinate to the AuNP surface to help displace the surface citrate, resulting in a more charge neutral surface. Alternatively, if this position is not adsorbed, it may serve as a hydrogen bond donor to interact with a ligand on another AuNP to induce aggregation. These roles either decrease charge repulsion or increase interparticle attraction, both promoting AuNP aggregation.

SERS to study adsorption

For both stabilization and destabilization interactions, the likely cause is the adsorption of the target onto the AuNPs. To further verify adsorption, surface-enhanced Raman scattering (SERS) was performed for caffeine, theophylline, and xanthine (Figures 6B–D). Compared to the free molecules in water, the SERS samples with AuNPs had much stronger signals despite their concentrations being 10-fold lower, confirming adsorption. The Raman spectra obtained were consistent with literature values for xanthine peaks. In work done by Muniz-Miranda to study xanthine using Raman spectroscopy and silver nanoparticles, enhanced peaks at around 657 cm^{-1} were observed.⁵⁵ In Figure 3C, we also observed a strongly enhanced peak at approximately 657 cm^{-1} , which solidly suggested adsorption of xanthine onto the AuNPs. The Raman spectra for caffeine also suggested adsorption, which is given by the enhanced peak at approximately 555 cm^{-1} (Figure 3B).⁵³ Theophylline results are indicative of adsorption as well, as evidenced by the peaks at 555 cm^{-1} and 1570 cm^{-1} (Figure 3D).⁵⁴ These results strengthened our hypothesis, supporting that the stabilization or destabilization interactions with AuNPs were afforded due to the adsorption of our targets onto the AuNPs.

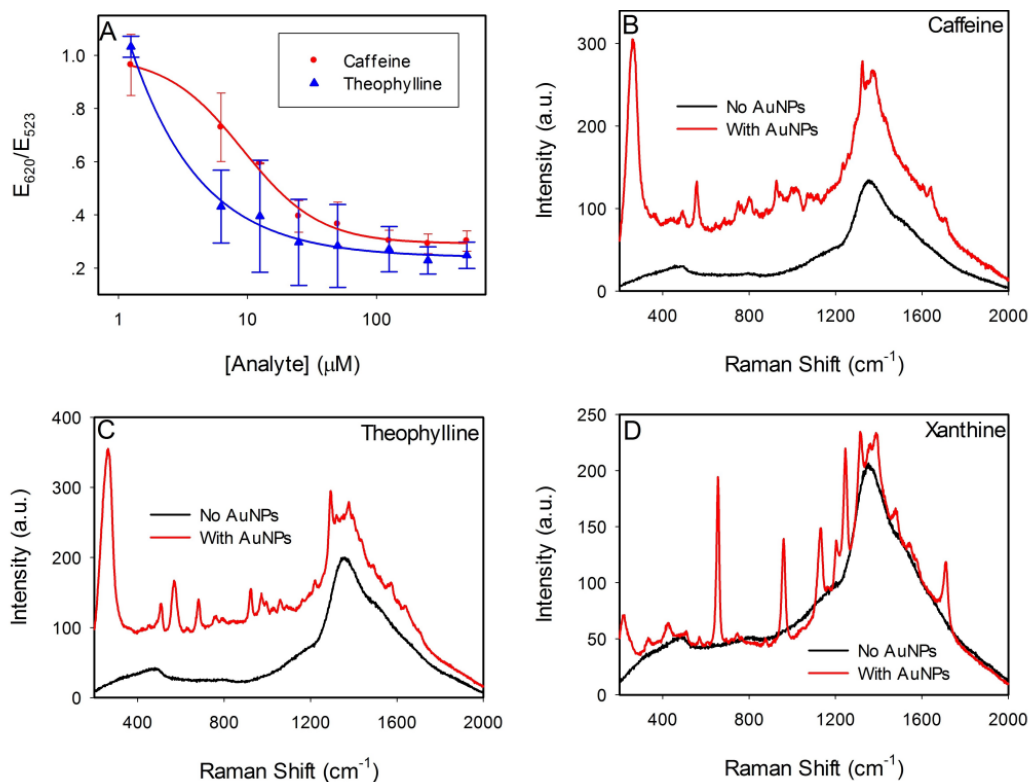


Figure 6. (A) Protection of AuNPs offered by caffeine and theophylline. Samples were prepared using 3nM AuNPs with a final of 40mM NaCl added. SERS spectra of (B) 5 mM caffeine alone, and 0.5mM caffeine with 100nm AuNPs and 1.2mM MgSO_4 , (C) 0.5mM xanthine alone, and 0.05mM xanthine with 100nm AuNPs and 1.2mM MgSO_4 , (D) 5mM theophylline solution, and 0.5mM theophylline with 100nm AuNPs and 1.2mM MgSO_4 .

Protection of AuNPs by the aptamers.

For the sensing method to work as intended, aptamers must be able to protect the AuNPs against salt-induced aggregation. Figure 7A and 7B illustrate the predicted secondary structures of the caffeine and theophylline aptamers, respectively. To ensure that the aptamers were suitable for the sensing method, preliminary experiments were done to verify the protection. As the concentration of the aptamer increased, the ratio of absorbance decreased proportionally (Figure 7C), confirming that these aptamers can indeed protect the AuNPs. Protection was observed at each of the studied concentrations to varying degrees. Protection

reached a plateau at around 100nM, for both the caffeine and theophylline aptamers. Given these results, 100nM aptamer concentrations were used for subsequent experiments.

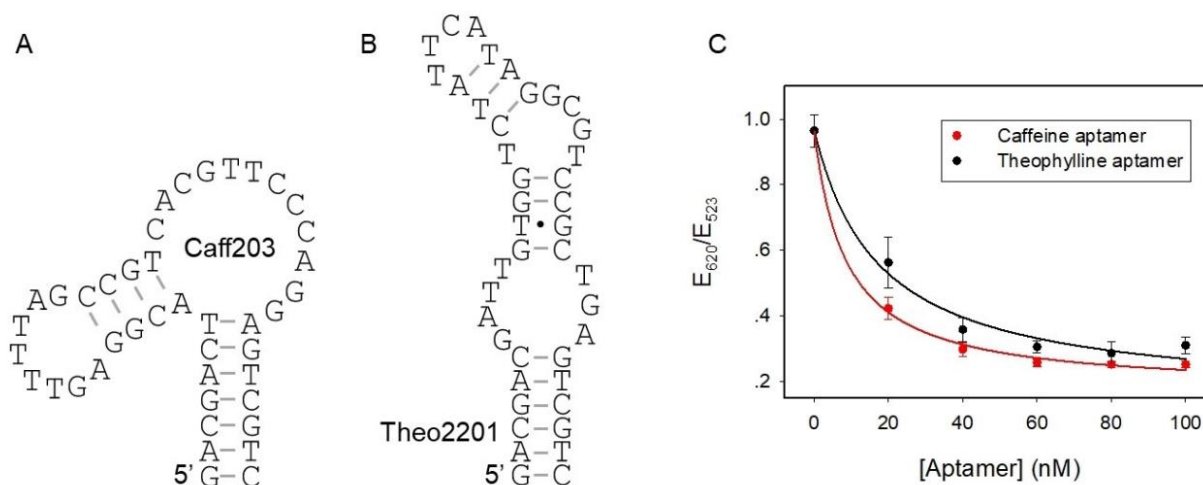


Figure 7. The secondary structure of the (A) caffeine and (B) theophylline aptamers. (C) Protection against salt-induced aggregation offered by caffeine and theophylline aptamers.

Label-free colorimetric sensing of caffeine and theophylline

Single-stranded DNA molecules can interact with the surface of AuNPs in a way that stabilizes the AuNPs. This interaction is due to the nitrogenous lone pairs that are present on nucleobases. NaCl destabilizes AuNPs by screening the surface charge, such that aggregation ensues. The typically proposed sensing mechanism makes use of these two interactions to determine whether an aptamer sequence is binding to a particular target. Specifically, when both DNA and NaCl are present, the protective, or stabilizing, effect of DNA is dominant, and thus the AuNPs are protected against salt-induced aggregation. However, when the target of said aptamer is included in the system, the aptamer will preferentially interact with the target, thus reducing or eliminating the protective effect of the aptamer for the AuNPs (Figure 8A).

Following the method in Figure 8A, we tested the detection caffeine and its derivatives using the caffeine and theophylline aptamers. Given that in the samples shown in Figure 8B and 8C, NaCl had thus far not been added, yet aggregation was observed for some molecules, it becomes evident that the target-AuNP interaction was predominating in those cases. If DNA-AuNP were the primary interactions in the system, there would be no aggregation before the addition of salt. Aggregation prior to salt addition means that the target can induce aggregation of the AuNPs regardless of the presence of aptamers.

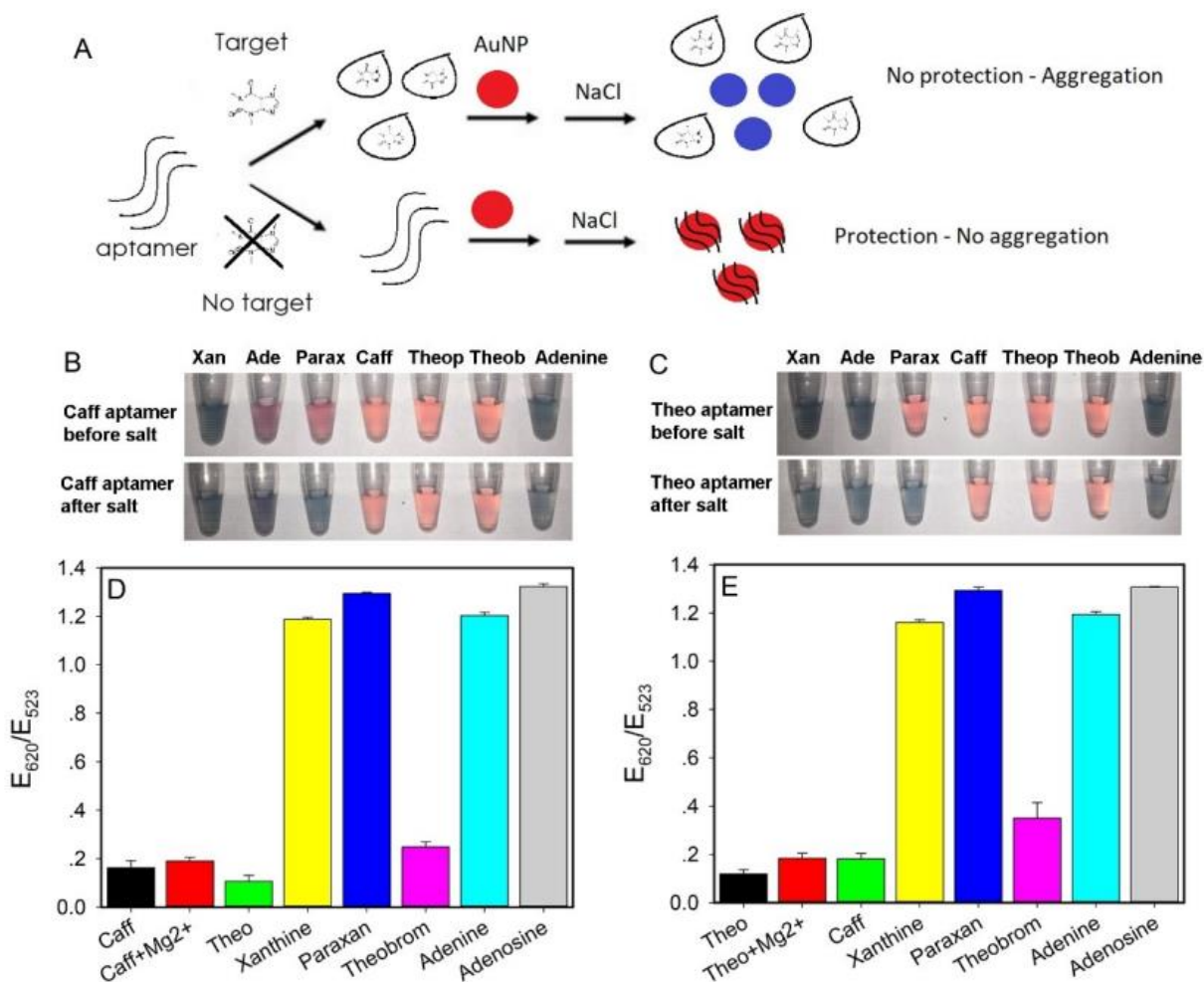


Figure 8. (A) The conventional mechanism for the label-free sensing method. In this mechanism, only the adsorption of aptamers is considered, while the adsorption of target molecules is not considered. Photographs of sensing results using the (B) caffeine aptamer and

(C) theophylline aptamer before and immediately after adding NaCl. Samples consisted of 1 mM phosphate buffer, pH 7.3, 4nM AuNPs, 10 μ M target, 100nM DNA aptamer, and 0 or 40mM NaCl. Quantified sensing assay results with caffeine (D) and theophylline (E) aptamers after adding 40mM NaCl. For the samples with Mg²⁺ added, 0.5mM Mg²⁺ was used.

As further evidence for the dominance of the target-AuNP interaction, neither caffeine with the caffeine aptamer (Figure 8D), nor theophylline with the theophylline aptamer (Figure 8E) samples showed aggregation upon the addition of salt. This again shows that it is the target that is interacting with AuNPs more strongly, as no aggregation is observed where it is expected to occur due to the protection against salt-induced aggregation offered by caffeine and theophylline. For each of the samples shown in Figures 8B–E, aggregation is shown to be based on the interaction of the target with AuNPs (i. e., those targets that were shown to induce aggregation in previous assays are again showing aggregation in the sensing experiment here, and those that were shown to offer protection against salt-induced aggregation in previous assays are showing no discernable change in absorbance ratio following the addition NaCl).

Further tests were done to assess whether a higher concentration of salt may alter the results. Concentrations up to 100mM NaCl were assayed (Figure 9). These assays showed that the sensing result was dependent on the presence versus absence of theophylline – assays were done with just theophylline, theophylline and aptamer, and just aptamer (each with NaCl and AuNPs). For each assayed concentration of salt, the sensing results mirrored the theophylline-only result, suggesting that the theophylline-AuNP interaction is dominant in the system, regardless of the NaCl concentration used.

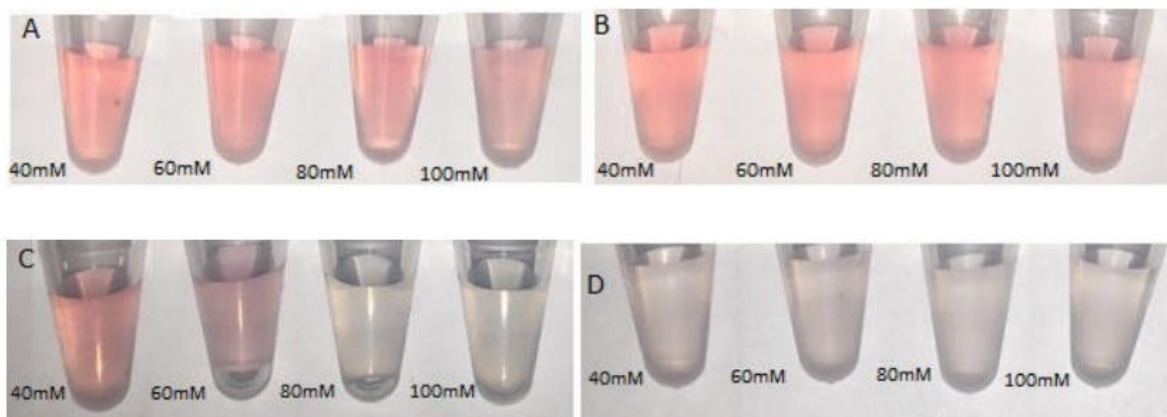


Figure 9. Alternate sensing experiments to assess whether varying the salt concentration may alter the results. AuNPs and NaCl were present in each system. (A) Only theophylline was added. (B) Assays with theophylline and theophylline aptamer together. (C). Assays where only the aptamer was included. (D) Neither theophylline nor aptamer were added. Concentrations to the left of each sample give the concentration of NaCl used in that system.

Even more, $MgCl_2$ was added to the caffeine aptamer sample to promote aptamer-target binding. However, despite adding $MgCl_2$, still no aggregation was observed for the caffeine with caffeine aptamer sample (Figure 8D). The same can be said for the sensing assay with the theophylline and theophylline aptamer, which also included 0.5mM $MgCl_2$ (Figure 8E). Increasing $MgCl_2$ further was not possible, as higher concentrations of Mg^{2+} can readily induce aggregation of the AuNPs.

Therefore, based on this sensing assay, this system was dominated by target/AuNP interactions. If the DNA-AuNP interaction dominates, the samples with targets that do not bind the aptamer should not show any aggregation, and the targets which bind to the aptamer will show aggregation once NaCl had been added. If the target-gold interaction dominates, then aggregation will depend solely on the stabilization/destabilization interaction of the target with

AuNPs. Prior to adding NaCl, aggregation is already seen in the samples with xanthine, adenosine, and adenine. Because the paraxanthine samples aggregated slower than other aggregation-inducing targets, paraxanthine kinetics experiments were done (Figure 10). These experiments showed that aggregation began between 5–10 min after adding paraxanthine to the AuNPs, and full aggregation ($E_{620}/E_{523} > 1.0$) was reached at approximately 30 min.

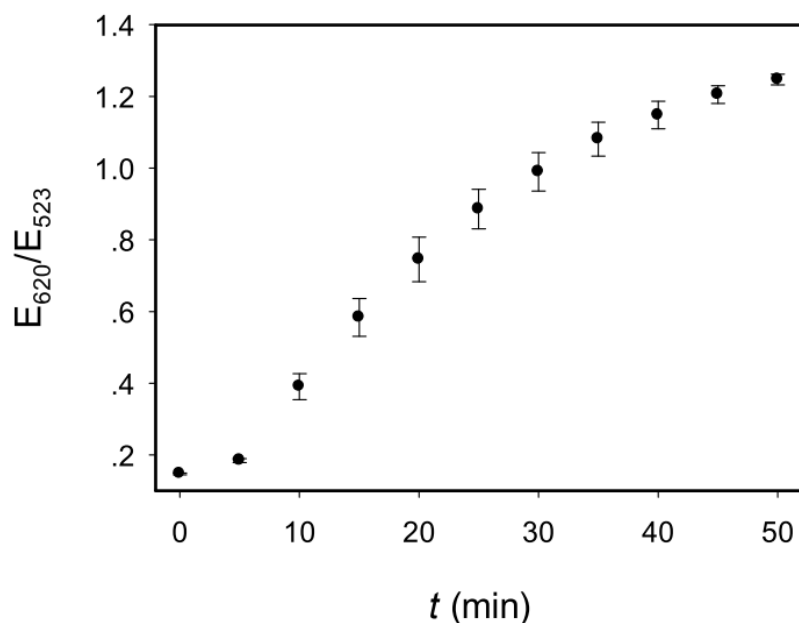


Figure 10. Paraxanthine-induced AuNP colour change kinetics. Experiments were repeated three times. Samples were made to mimic the sensing conditions – approximately 4nM AuNPs and 10 μ M paraxanthine were used. Measurements were taken using UV Vis spectroscopy every 5 min, for 50 min; $E_{620}/E_{523} \geq 1.0$ is used as a reference for “complete” aggregation, as it is the approximate ratio of absorbances for AuNPs that have been aggregated by NaCl. Further increases in the ratio of absorbances are due to the shift from a purple to blue appearance of the nanoparticles.

Based on whether target molecules can adsorb and whether DNA can bind to target, there are four possibilities as summarized in Figure 11. In Figure 11B and 11D, we are getting

the 'expected' result – aggregation when target of interest is present, and no aggregation when a non-target is present. However, despite these being the expected results, the underlying mechanism can be different from previously reported. Previous iterations of this sensing method conclude that aggregation occurs because no protection against salt-induced aggregation is being afforded by DNA, when in-fact we would see aggregation prior to adding salt. This indicates target-induced destabilization of the AuNPs (as suggested in Figure 11D). As well, there is potential for both false-negative and false-positive results, as shown in Figure 11A and 11C. In Figure 11A, despite there being DNA-target binding, no aggregation is observed because of the stabilization effect of the target. The conclusion would be that no binding is occurring, when in fact it is simply being masked. Alternatively, Figure 11C shows a false-positive – it appears as though binding is occurring, though aggregation ensues before salt addition because of the destabilizing effect of the target.

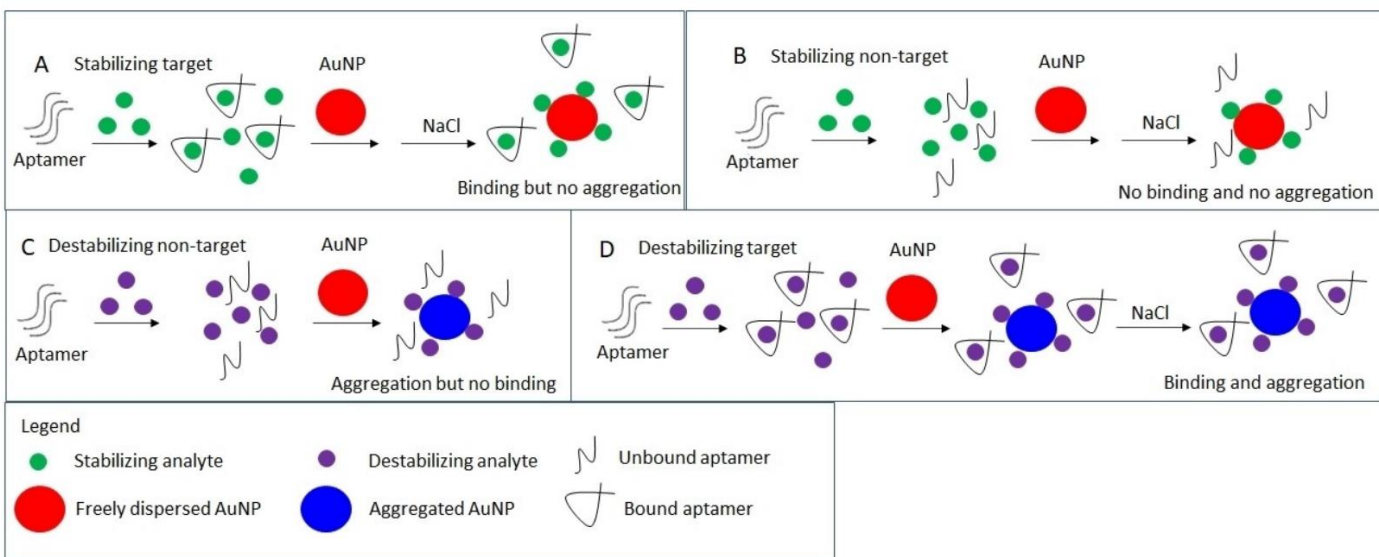


Figure 11. Possible results for the sensing assay when the target is dominating in the system. (A) The expected results when a stabilizing target is used. (B) The expected results when a

stabilizing non-target is assayed. (C) The expected result when a destabilizing non-target is used, and (D) the expected result when a destabilizing target is assayed.

Considering results reported here, and the described potential results, previous work that made use of this method may need to be revisited to ensure the validity of the conclusions. For instance, this method has been used as proof of successful aptamer selection for a number of sequences.²³ Because of the stringency required for success, these sequences may need to be studied using alternate methods to ensure their viability. An example where the constraints not being met did in fact lead to false conclusions is shown in work done by Zong et al.²⁴ This false conclusion came about partially due to the failure to report target-gold interactions between arsenic and AuNPs.²⁵ For this method to be successful as it has been intended,⁵¹ three primary constraints should be met: 1) NaCl must be the only component in the system which can induce the aggregation of AuNPs; 2) the DNA aptamer must be able to protect against salt-induced aggregation, and it must be the only component in the system which can do so; 3) the target in question must not interact with AuNPs in either a stabilizing nor a destabilizing manner. If such an interaction were to exist, it must be weaker than the interaction of DNA with AuNPs.

Conclusions

In this work, we studied the adsorption of caffeine and theophylline by AuNPs and evaluated the feasibility of aptamer-based label-free detection. Adsorption was observed based on the colloidal stability of AuNPs and Raman spectroscopy, and due to such adsorption, the AuNPs could not be used for direct label-free colorimetric detection. Future research on more reliable methods for detection and quantification of small molecules using AuNPs would need

to carefully consider target-gold interactions. Alternate methods with less constraints for success can be explored. Results presented in these works also suggest that the method as reported should not be used as proof of aptamer binding, and alternate binding assays should be employed when reporting new aptamer sequences.

Experimental Section

Chemicals: The 13 nm AuNPs were used for all assays other than Raman spectroscopy. The 13 nm AuNPs were prepared according to literature.⁵⁷ A 1 mM HAuCl₄ solution was heated to refluxing, and then a 1% Na₃C₆H₇·2H₂O was added to the refluxing solution. This was allowed to react until a wine-red color was achieved; the solution was then slowly cooled. DNA samples were purchased from Integrated DNA Technologies (Coralville, IA, USA). The caffeine aptamer sequence is 5'-GAC GAC TAC GGA GTT TTA GCC GTC ACG TTC CCA GGA GTC GTC-3', and the theophylline aptamer sequence is 5'-GAC GAC GAT TGT GGT CTA TTC ATA GGC GTC CGC TGA GTC GTC-3'. Sodium chloride, 4-(2-hydroxyethyl) piperazine-1-ethanesulfonic acid (HEPES), MES, NaH₂PO₄, Na₂HPO₄, KH₂PO₄, caffeine, theophylline, xanthine, paraxanthine, theobromine, adenine and adenosine were purchased from Sigma-Aldrich. Milli-Q water was used to prepare all the solutions and buffers.

AuNP stability assays: To assess the effect of the target molecules on the stability of the AuNPs, titrations were made to a final concentration of 3nM AuNPs, and target concentrations ranged from 1μM to 2mM. Reactions consisted of 55μL of AuNPs and 55μL of respective target solution. For consistency, samples were allowed to sit for 1 h at room temperature before measurements were taken on a UV-Vis spectrophotometer. For pH studies, a

carbonate/bicarbonate buffer was used for pH 10.2, and a sodium phosphate/potassium phosphate buffer was used for pH 4.2.

Aptamer-based sensing: Protection offered by the chosen aptamer sequences was first assessed by aggregation experiments. An approximately 4nM final concentration of AuNPs was used, with aptamer concentrations ranging from 20–100nM. Samples were made up of 70 μ L AuNPs, 10 μ L of the respective DNA solution, and 20 μ L of NaCl (40mM final). The sensing experiments were done by first mixing the aptamer with target and were left to interact for 5 min; a 5mM phosphate buffer, pH 7.3 was used for this reaction. Next, AuNPs were added, and results were photographed. Finally, NaCl was added to each of the samples and results were again photographed and recorded using UV-Vis spectrometry. The final concentrations of the reactants were 100nM DNA, 10 μ M target molecules, 40mM NaCl, 1mM phosphates buffer, and approximately 4nM AuNP. The final sample volume was 100 μ L, which consisted of 60 μ L AuNPs, 10 μ L aptamer solution, 10 μ L target, and 20 μ L NaCl. Alternate salt concentrations were assayed for the sensing experiments with theophylline. 10 μ M theophylline, 100nM theophylline aptamer, and 4nM AuNP concentrations were used; NaCl concentrations ranged from 40mM to 100mM.

SERS and UV-vis Spectroscopy: Samples were prepared using 100nm AuNPs prepared by citrate reduction. The final caffeine, theophylline and xanthine concentrations were 0.05 to 0.5mM, and 1.2mM MgSO₄ was used when needed, to aggregate the AuNPs to increase Raman

hotspots. For the AuNP-free spectra, the concentration of the molecules was 10-fold higher. Measurements were taken using a DeltaNu Advantage 785 Raman spectrophotometer, with an excitation wavelength of 785nm and an integration time of 5s. All UV-vis spectrophotometry results were obtained using an HP/Agilent 8453 UV-Vis spectrophotometer.

Chapter 3 - Graphene Oxide-Induced Quenching of Fluorescently Labelled Aptamers for Fluorescence-Based Detection of Caffeine and Theophylline

Introduction

Pertaining to small molecule detection, a target that is quite often studied is adenosine.⁵⁸⁻⁶⁰ Although adenosine is a biologically important molecule, it is important to study potential sensing mechanisms for other small molecule targets. In particular, because of their biological and pharmaceutical importance, we are interested in determining simple, cheap, and reliable ways to detect the important methyl-xanthines caffeine and theophylline.

Caffeine is the most abundantly used psychoactive substance in North America.¹² Although many studies have shown that in general, caffeine consumption does not have any negative health effects in the average healthy adult individual, there have been some recent concerns regarding the contamination of coastal ecosystems by this molecule.³⁵ This contamination has arisen due to its high prevalence in human consumption. Because of this, being able to detect it reliably and specifically is important for ensuring that contamination does not approach an environmentally impactful concentration.

Theophylline is a molecule with therapeutic importance, which makes its detection also of interest. In particular, it is used for the treatment of airway diseases, such as asthma.^{40,42-43} Theophylline is also a main active component in tea, and is present in other consumable products, such as chocolate. Despite this, however, it is possible to overconsume theophylline in a way that is harmful to one's health. Because of this, it is important to be able to accurately

monitor concentrations of theophylline, with potential applications in medical practices, or for monitoring environmental concentrations, should the need arise.

A potential mechanism for sensing these targets makes use of graphene oxide (GO). GO can interact and bind strongly with single stranded DNA molecules, like aptamers, due to π -stacking, as well as hydrophobic interactions between graphene and the nucleobases of DNA.^{8,34,60} In addition, GO can induce fluorescence quenching of fluorophores – when a fluorescently labelled aptamer adsorbs onto graphene oxide, this interaction causes an alteration of the structure of the aptamer that inhibits fluorescence. As the aptamer is released from the surface of the GO lattice, it regains its fluorescence – i.e., we get enhancement.³⁰⁻³² Enhancement occurs as a result of the aptamer returning to its native structural conformation upon dissociation.

Though there exists a variety of fluorescent labels, FAM was chosen as our label for these methods, as it is an inexpensive option, and it is small, which helps to ensure that the inclusion of the label on the aptamer structure will not alter the structure in a way that prevents binding of our aptamer to its target.²⁷⁻²⁸

The idea behind the sensor is that graphene oxide can induce high levels of fluorescence quenching of our chosen fluorescent label. Once the target of the aptamer has been added, fluorescence enhancement will ensue, as a result of the aptamer binding preferentially with its target instead of interacting with graphene oxide.

Additionally, double stranded DNA cannot interact with graphene oxide because the nucleobases are interacting with their complimentary strand, and essentially “hidden away”

from the GO surface.³⁰⁻³² Because of this, we used an aptamer and its complimentary (cDNA) strand as a control for our experiments. When complimentary DNA is introduced into the sample, the aptamer will preferentially bind to the cDNA. Since double stranded DNA cannot adsorb onto GO, the newly double stranded DNA remains dissociated, which allows fluorescence enhancement.

Results and discussion

Both graphene oxide and the DNA backbone carry a negative charge. Because of this, a buffer with high ionic strength was needed, in order to mitigate the repulsive energy that exists as a result of these negative charges. To this end, both MgCl_2 and NaCl were included – their positively charged ions (Mg^{2+} and Na^+) serve to screen the negative charges on the reactants, DNA and GO. Additionally, the FAM fluorophore requires a near-neutral/neutral pH to fluoresce, so a pH 7.5 HEPES buffer was also included in the samples.²⁷

First, the caffeine aptamer and the theophylline aptamer were assayed with both caffeine and theophylline; these samples included buffer, aptamer, NaCl , MgCl_2 and (7.5 $\mu\text{g}/\text{mL}$) GO. These initial experiments showed that for the caffeine aptamer, adding caffeine resulted in a fluorescence signal equal to $4.07x \pm 1.1x$ of the baseline. In comparison, adding theophylline to the caffeine aptamer mixture resulted in fluorescence enhancement equal to $2.24x \pm 0.4x$ the baseline. Each of the increases reported were determined using the maximum fluorescence obtained when monitored for a 30-minute period after adding target. These results showed that greater enhancement was shown to specific dissociation of the caffeine aptamer by its target. These results are shown in Figure 13.

To calculate the enhancement, prior to adding target the samples were monitored for 5 minutes. The values obtained during this analysis were then averaged out – this average value was used as the baseline. After adding target, the samples were monitored for 30 minutes. The maximum R. F. U. (relative fluorescence units) value was used to compare to the baseline. The enhancement value was calculated as $\frac{\text{Max RFU after target}}{\text{Average RFU before target}}$; with this, the values given, for example caffeine with its aptamer, as 4.04x demonstrated that after adding target, the R. F. U. is equal to 4.04 times the magnitude of the pre-target baseline fluorescence.

Similarly, when caffeine was added to the theophylline aptamer samples, there was a fluorescence output equal to $3.27x \pm 0.3x$ the baseline within 30 minutes. When theophylline was added to the sample containing its aptamer, there was an average maximum fluorescence output of $2.9x \pm 0.3x$ the baseline (Figure 14). Like the caffeine aptamer results, there was a greater average enhancement when caffeine was added to the theophylline aptamer samples. This indicates that caffeine likely induces better non-specific displacement of the aptamer from the graphene oxide surface when compared to theophylline.

To determine whether this assertion was true, both caffeine and theophylline were assayed as the non-specific targets for a FAM-labelled 24-mer sequence. Because the 24-mer sequence has a lower fluorescence when freely dispersed when compared to the FAM caffeine and theophylline aptamers, a lower (optimized) concentration of GO ($5\mu\text{g/mL}$) was used for these experiments. When compared to the dissociation of their respective aptamers, results showed that, once again, caffeine caused a greater degree of nonspecific dissociation of the

DNA from GO (Figure 12). This further confirms the hypothesis that caffeine can cause nonspecific displacement of DNA more readily than theophylline.

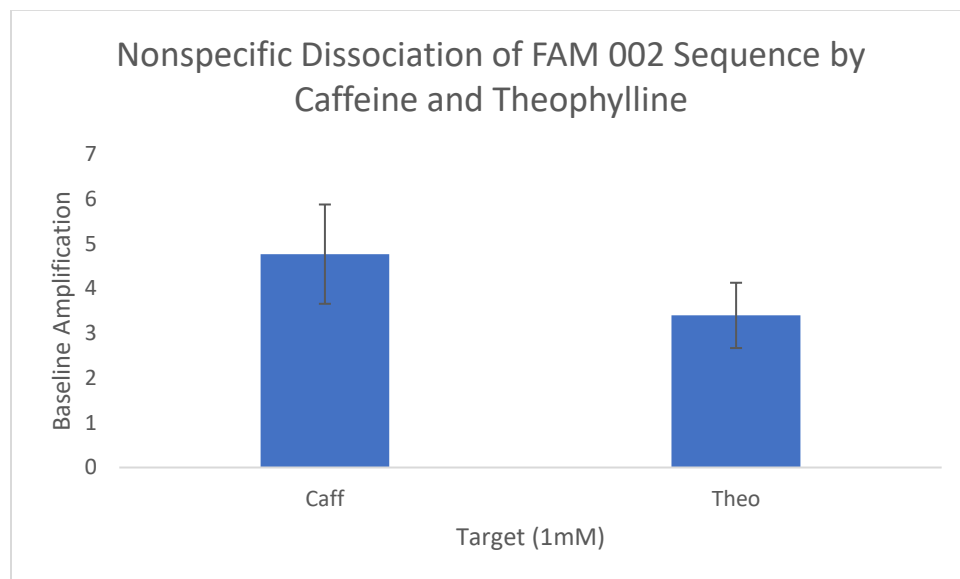


Figure 12. Visualized results of the nonspecific dissociation of a 24-mer DNA sequence by our targets, caffeine (caff) and theophylline (theo). Both targets were assayed using 1mM concentrations, DNA was 20nM and GO was 5 μ g/mL.

Effect of BSA

Bovine serum albumin, or BSA, is often used for the purpose of “blocking” in conditions where non-specific displacement is possible.⁶¹⁻⁶² The purpose of BSA is to prevent non-specific displacement of our aptamer, by essentially “filling” the sections of the GO lattice that are not occupied by the aptamer. In doing so, when the target is added, the chances that the target binds preferentially to GO are decreased, allowing for a higher increase in fluorescence upon their addition. Figures 2 and 3 show how the inclusion of BSA (0.004mg/mL) in our sensors served to increase the target-induced fluorescence enhancement for both the specific and nonspecific targets.

BSA was assayed with each aptamer, but results showed that despite it improving the fluorescence enhancement of the specific targets, it also increased the signal of the nonspecific target. These results indicate that the inclusion of BSA helped with the sensitivity of the sensor, but was a detriment to the selectivity, and thus was excluded from sensing experiments after initial assays.

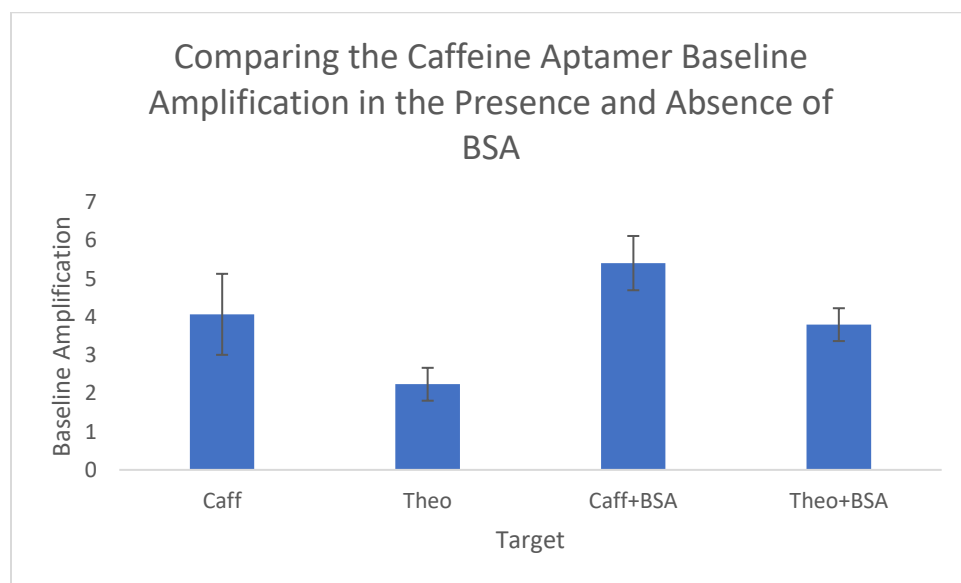


Figure 13. To compare the amplification of fluorescence output when BSA is present versus absent. The caffeine aptamer with caffeine had $4.07x \pm 1.06x$ the baseline without BSA and $5.41x \pm 0.71x$ with BSA. When theophylline was added, amplification was $2.24x \pm 0.43x$ without BSA and $3.8x \pm 0.43x$ with BSA.

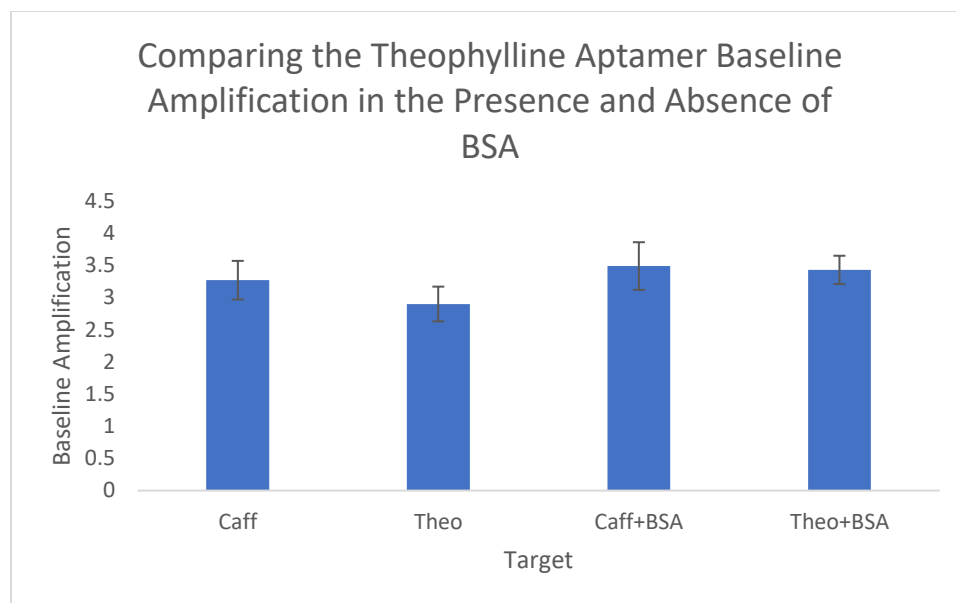


Figure 14. To compare the amplification of fluorescence output when BSA is present versus absent. The theophylline aptamer with theophylline had $2.9x \pm 0.3x$ the baseline without BSA and $3.43x \pm 0.2x$ with BSA. When caffeine was added, amplification was $3.27x \pm 0.3x$ without BSA and $3.49x \pm 0.4x$ with BSA.

Although the addition of BSA reduced the difference in amplification between theophylline and caffeine when each was added to the theophylline aptamer, caffeine still showed greater fluorescence enhancement in both assays. This leads to the conclusion that the sensing method designed and discussed here does not work for the FAM labelled theophylline aptamer.

Verification of Method Design

To assess whether the method proposed here was correctly designed and confirm that the caffeine and theophylline results were due to the method not working for these aptamers, rather than due to a flaw in the sensor, an alternate DNA sequence was used. The 24-mer sequence has a complimentary DNA strand, that can be used as a specific target for the sensor. As a nonspecific target, the same 24-mer sequence, just unlabelled, can be used.

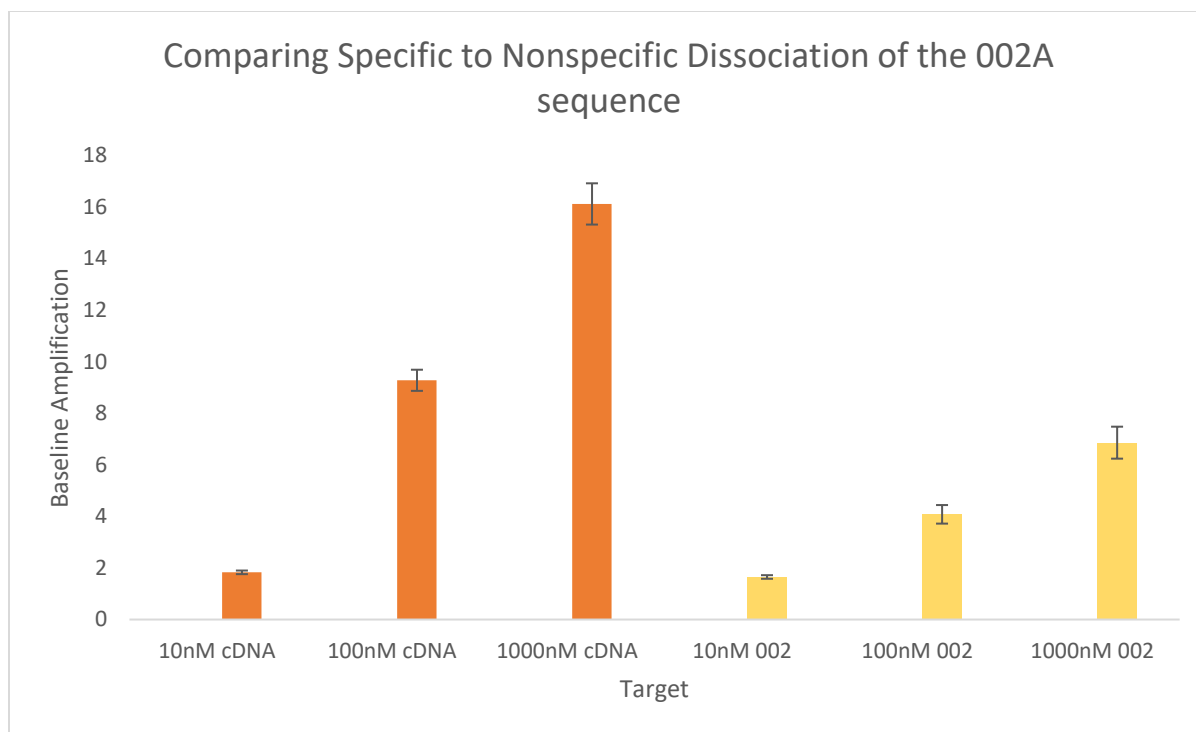


Figure 15. Comparison of specific and nonspecific dissociation of the FAM 24-mer sequence using DNA targets.

As shown in Figure 15, when the concentration of the specific target increased, so did the resulting RFU. A similar trend was shown for the nonspecific target, though the amplification at each concentration differed significantly. Specifically, the cDNA target showed $1.83x \pm 0.1x$, $9.28x \pm 0.4x$, and $16.12x \pm 0.8x$ amplification at 10nM, 100nM and 1000nM target, respectively. In comparison, when the unlabelled 002 sequence was added as the target, we saw $1.65x \pm 0.1x$, $4.08x \pm 0.4x$, and $6.86x \pm 0.6x$ for 10nM, 100nM and 1000nM target concentrations. These results clearly show success of the method, as the nonspecific target results in significantly lower enhancement than the specific target. This suggests that the method works as intended, and that the caffeine and theophylline aptamers are simply non ideal candidates for using this sensing mechanism.

Non-specific displacement

Adenosine

Experiments for the nonspecific displacement of the caffeine and theophylline aptamers showed that similar targets were able to displace the aptamers almost as readily as the specific targets. To determine whether the structure of the target may be related to nonspecific dissociation, we decided to study another nonspecific target that has greater structural differences compared to the specific targets for our aptamers. To this end, adenosine (1mM) was used as the nonspecific target; each of their structures is pictured below.

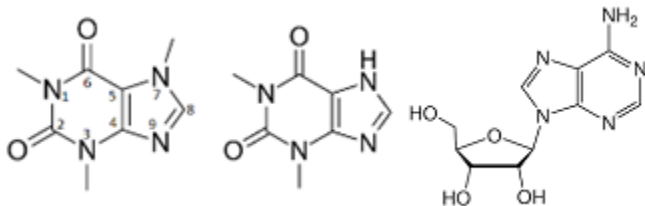


Figure 16. Structures of each of our small molecule targets, from left to right : caffeine, theophylline, adenosine.

Caffeine and theophylline differ by only a single methyl group, whereas adenosine is much larger, containing an additional ring as part of its structure.

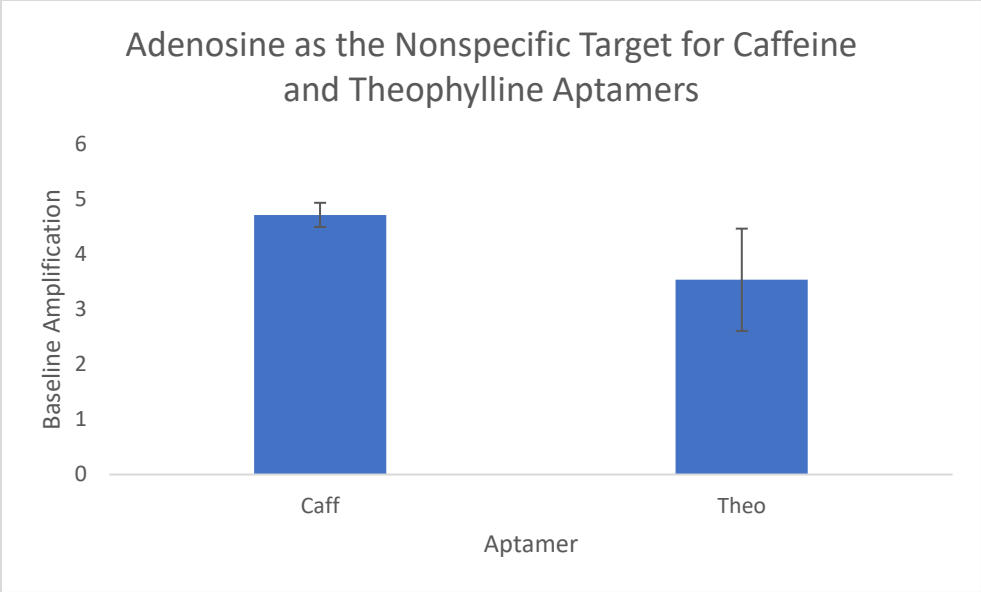


Figure 17. Nonspecific dissociation of caffeine and theophylline aptamers using adenosine as the target. Assayed with the caffeine aptamer, adenosine induced an RFU that was equal to $4.72x \pm 0.22x$, and an RFU equal to $3.54x \pm 0.93x$ the baseline when assayed with the theophylline aptamer.

Next, we also wanted to determine how these results differed from each of these targets assayed with the adenosine aptamer.

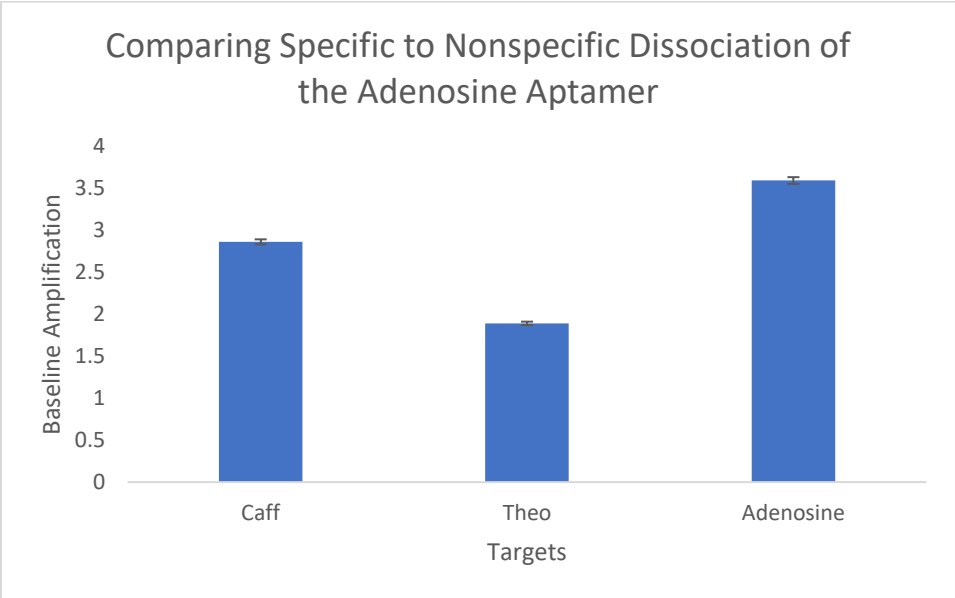


Figure 18. Dissociation of the adenosine aptamer from GO by caffeine, theophylline and

adenosine. Each target was assayed using a concentration of 1mM. Caffeine induced an amplification of $2.86x \pm 0.03x$, theophylline $1.89x \pm 0.02x$, and adenosine $3.59x \pm 0.04x$.

Looking at the results shown in Figure 18, we find that adenosine was able to induce a greater fluorescence enhancement when assayed with its aptamer, when compared to caffeine and theophylline. Interestingly, the amplification given when adenosine was assayed with the caffeine aptamer was higher than the amplification observed when adenosine was assayed with its own aptamer. These results suggest that the amplification of fluorescence, though likely correlated with binding of aptamer to target, appears more highly dependent on the target being used, and how that target may be interacting with GO. Additionally, the strength of the interaction between the aptamer and GO may influence the resulting fluorescence enhancement.

Concentration dependence

Concentration dependence for each target with both aptamers was studied, to determine how sensitive the proposed sensing mechanism is for specific and non-specific displacement. Results showed a threshold of detection of $10\mu\text{M}$ for caffeine with the caffeine aptamer, $100\mu\text{M}$ for caffeine with the theophylline aptamer, and $100\mu\text{M}$ for theophylline with both aptamers. The threshold of detection is given as the concentration assayed where the fluorescence is great than 1.0x the baseline. Results are presented in Figures 19 and 20.

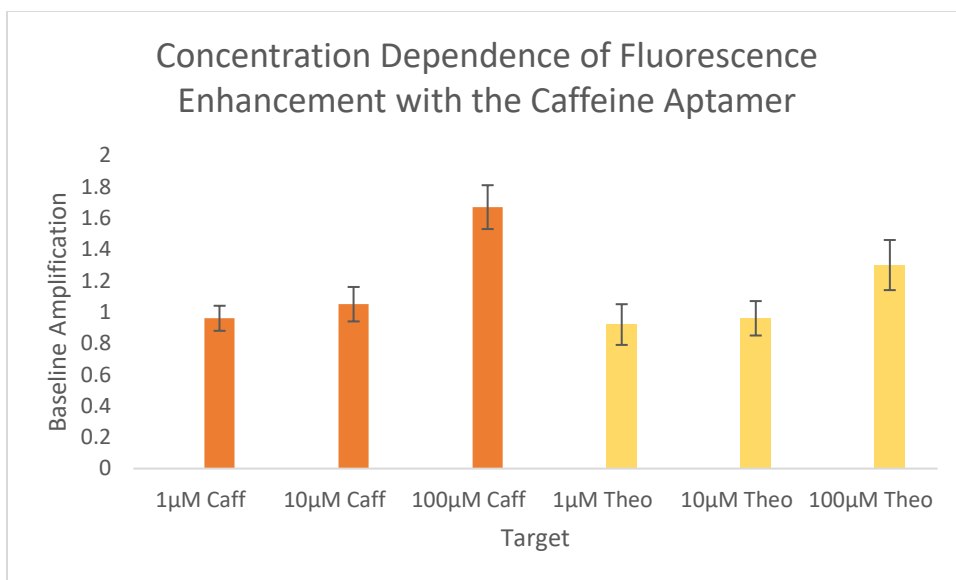


Figure 19. Concentration dependence of the fluorescence enhancement of the caffeine aptamer. Caffeine as the target gave enhancements of $0.96x \pm 0.08x$, $1.05x \pm 0.11x$, and $1.67x \pm 0.14x$ with concentrations of $1\mu\text{M}$, $10\mu\text{M}$, and $100\mu\text{M}$, respectively. Theophylline as the target showed enhancements equal to $0.92x \pm 0.13x$, $0.96x \pm 0.11x$, and $1.3x \pm 0.16x$ the baseline, with concentrations of $1\mu\text{M}$, $10\mu\text{M}$, and $100\mu\text{M}$, respectively.

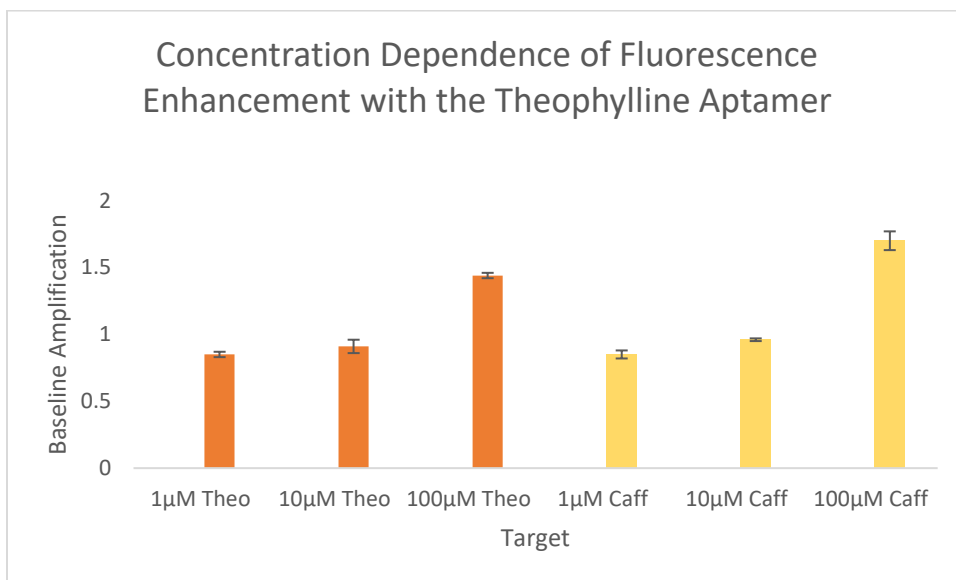


Figure 20. Concentration dependence of the fluorescence enhancement of the theophylline aptamer. Theophylline as the target gave fluorescence of $0.85x \pm 0.02x$, $0.91x \pm 0.05x$, and $1.44x \pm 0.02x$ with concentrations of $1\mu\text{M}$, $10\mu\text{M}$, and $100\mu\text{M}$, respectively. Caffeine as the targets showed fluorescence equal to $0.85x \pm 0.03x$, $0.96x \pm 0.01x$, and $1.7x \pm 0.07x$ the baseline, with concentrations of $1\mu\text{M}$, $10\mu\text{M}$, and $100\mu\text{M}$, respectively.

The concentration dependence experiments showed an increase in the fluorescence output that was only minimal in concentrations up to 100 μ M. These experiments were done to determine whether we would be able to observe a greater difference in the results for specific and nonspecific targets at lower concentrations. Results showed no significant difference at any of the lower concentrations that were assayed.

Target Effect on Fluorescence

The final experiments that were conducted were done so without including graphene oxide.

These were done to assess how the targets may be directly impacting the relative fluorescence; results are given in Figure 21.

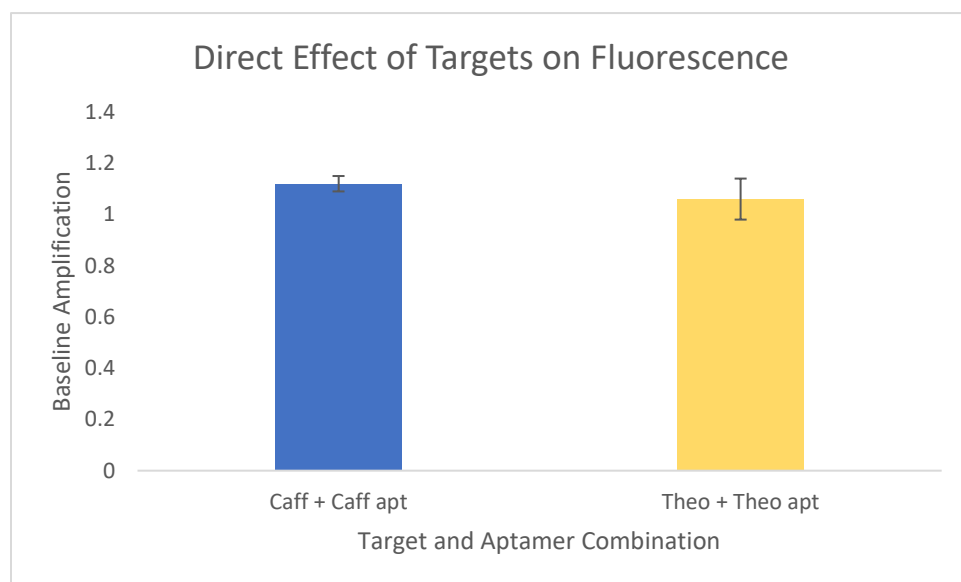


Figure 21. This figure shows how the target by itself affects the relative fluorescence. The samples of caffeine with the caffeine aptamer showed an average fluorescence of $1.12x \pm 0.03x$ the baseline. The samples of theophylline and theophylline aptamer showed an average fluorescence and $1.06x \pm 0.08x$ the baseline.

Results presented in Figure 21 suggest that the structure of the target being used in the sensor may have a direct effect on the fluorescence of a sample. Though no GO was used in these samples, adding each of the targets induced a small amount of fluorescence enhancement of the fluorophore. The actual cause of this change may be due to the structure of the target, and potential interaction with the aptamer or the fluorophore itself, though additional studies would be required to draw an exact conclusion.

Conclusions

The graphene-oxide based fluorescent sensor proposed here has the potential to be used for the detection of small molecules. It is, however, important that non-specific desorption of the aptamer of choice is studied thoroughly before using the method as described. The experiments reported in these works show that caffeine is able to displace aptamers from the graphene oxide surface quite well, suggesting a strong interaction between graphene oxide and caffeine. Studies with adenosine show such an interaction as well, with even higher levels of nonspecific dissociation than with caffeine. If no such interaction exists between GO and the target of interest, this method may be useful for future iterations of small molecule detection. Blocking with BSA was studied, as an attempt to improve the sensitivity and selectivity of the sensor. Despite the results showing an increase in sensitivity of the sensor, a decrease in the selectivity of the sensor was also observed. Further research on this topic could be done to determine if there is an alternative molecule that can be used as a blocker, to both improve sensitivity of the sensor, for a lower detection threshold, while also decreasing nonspecific binding, to maintain selectivity of the sensor.

Experimental section

Fluorescence analysis

Each of the fluorescence analyses presented were performed using a Tecan Spark fluorometer, with a gain value of 118. An excitation wavelength of 485nm was used, along with an emission wavelength of 535nm; this is the emission spectra of FAM that provided the least overlap between emission and excitation, allowing for more reliable data. The pH was maintained at 7.5, using a HEPES salt buffer.

Experimental conditions had probe DNA at 20nM, 20mM HEPES buffer (pH 7.5), 100mM NaCl, and 1mM MgCl₂. Each DNA, buffer, salts, and GO were mixed, and allowed to react for 30 minutes. Once 30 minutes had elapsed, 90µL of sample was measured on the fluorometer every 20s for 5 minutes; the average baseline fluorescence was recorded as the average fluorescence output of these 5 minutes. Finally, target was added to each sample, and fluorescence was monitored every 20s for 30 minutes.

The aptamer sequences used for these experiments were purchased from Integrated DNA Technologies. The sequence of the caffeine aptamer was 5' –GAC GAC TAC GGA GTT TTA GCC GTC ACG TTC CCA GGA GTC GTC – 3'

The sequence of the theophylline aptamer used was 5' –GAC GAC GAT TGT GGT CTA TTC ATA GGC GTC CGC TGA GTC GTC – 3'

The sequence of the 002 24-mer sequence was 5' ACG CAT CGA CAA AGA GAA CCT GGG 3'

The HEPES (4-(2-hydroxyethyl) piperazine-1-ethanesulfonic acid) salt, NaCl and MgCl₂, BSA and GO were purchased from Sigma-Aldrich. MilliQ water was used to make all salt solutions, samples, and buffers.

Optimization of Sensor Conditions – Order of Addition

The order of addition was optimized in tandem with the optimization of graphene oxide. In early iterations of these methods, the samples were reacted with GO while in the fluorescence reader plate. Although this allowed us to observe the kinetics of the interaction of GO with the aptamer, having the sample in the plate for extended periods of time caused a decrease in the fluorescence of the freely dispersed aptamer. This decrease was likely due to the adsorption of the aptamer onto the plate. Because of this, in further experiments, GO and aptamer were allowed 30 minutes to interact in a microfuge tube before fluorometry analysis. This served to decrease the time spent in the plate, thus decreasing unwanted adsorption of the aptamer to the plate itself.

Additionally, when BSA was used, it was added 30 minutes after adding GO. If BSA is added prior to the aptamer, GO may preferentially interact with BSA instead of the aptamer, causing a decrease in quenching, which would introduce too much undesired variability between samples.

Polyethylene glycol (PEG)

A problem that was consistently occurring in the first iterations of the sensor is that the control mix had decreasing fluorescence despite there not being any GO in the sample. The likely cause of this was the adsorption of the aptamer onto the fluorescence plate. To help mitigate this, PEG₂₀₀ (0.001%) was included, to act as a protective coat to prevent adsorption of the aptamer onto the plate.

Another way to mitigate the unintended decrease in fluorescence was to alter the order of addition. Kinetics experiments showed that the quenching by graphene oxide stabilized after approximately 30 mins; to avoid having the samples in the plates for more time than was necessary, a mix of all reactants was made, including graphene oxide, and was allowed to interact for 30 mins before any fluorescence measurements were taken.

Graphene oxide (GO) Optimization

The optimization of graphene oxide was done to determine the amount of GO needed to achieve approximately 90% quenching. If graphene oxide were added in excess, there would likely be interaction of the targets with the excess GO as opposed to with the aptamer as intended. If insufficient GO is added, then the background fluorescence would be too high, which decreases the accuracy and reliability of the results when adding our target.

To optimize graphene oxide, kinetics experiments were done, with conditions to mimic those intended for use in the sensor. This meant a reaction with an aptamer concentration of 20nM, a HEPES (pH 7.5) concentration of 20mM, 100mM NaCl and 1mM MgCl₂. Graphene oxide concentrations were varied from 1-4μL of 0.25mg/mL of GO per 100μL of sample. Concentrations were recorded as volumes for simplicity when optimizing the GO concentration. These experiments were done to determine how much GO was needed for the desired level of quenching, as well as the amount of time required for quenching to plateau.

Optimization experiments showed that the ideal concentration of graphene oxide for these aptamers was 2μL of GO per 100μL of sample (or 5μg/mL) for our 002 sequence, and 3μL per 100μL of sample (or 7.5μg/mL) for the caffeine, theophylline, and adenosine aptamers,

when using an aptamer concentration of 20nM. The caffeine, theophylline, and adenosine aptamers had higher baseline fluorescence for freely dispersed aptamer, and thus required a higher amount of GO in order to be quenched to the appropriate degree.

Bovine Serum Albumin (BSA) optimization

Like experiments for GO optimization, BSA optimization was done with conditions that mimicked those intended for use in the sensor. A control mix, that included all reactants other than GO was made for comparison. GO mixes were made, which consisted of 20mM HEPES, 100mM NaCl, 1mM MgCl₂, and 7.5µg/mL GO as the final concentrations; mixes were made to have a volume of 450µL, to be topped up to 500µL total, once BSA was added (concentrations shown are calculated assuming a 500µL final volume).

Samples were first allowed to react with graphene oxide for 30 minutes. Once 30 minutes had elapsed, samples were measured for five minutes on the fluorometer to create a baseline for comparison; finally, 10µL of BSA was added to each of the samples of GO mix, which were then measured on the fluorometer for 30 minutes.

The optimal concentration of BSA is one that induces only a minimal increase of fluorescence. The reason for this is that we want to determine how much BSA is needed to “fill” the empty spaces on the graphene oxide lattices left by our aptamer. If too much BSA is added, we will get a large increase in fluorescence, meaning that a large amount of aptamer has been displaced from the surface of GO. If insufficient BSA is added, we will observe no signal change, which indicates that there are still empty spaces on the surface of our GO lattices where the target may be able to adsorb. The adsorption of our target onto the GO surface can alter the concentration of target needed to observe a change in fluorescence. Ideally, the least amount

of target that adsorbs onto the GO, the lower the detection limit will be. Blocking offered by BSA has the potential to also help decrease nonspecific dissociation of our aptamer.

BSA optimization and kinetics experiments showed that BSA-induced fluorescence enhancement stabilized 45 minutes after addition. Thus, when BSA was used, samples were allowed to react for 45 minutes before fluorescence was measured.

References

- [1] Michelmore, A. Thin Film Growth on Biomaterial Surfaces. *Thin Film Coatings for Biomaterials and Biomedical Applications* **2016**, 29-47
- [2] Sun, H., Zu, Y. Aptamers and Their Applications in Nanomedicine. *Small* **2015**, 20, 2352-2364.
- [3] Lowe, C. R. Biosensors. *Trends in Biotechnology* **1984**, 2, 3, 59-65
- [4] Saha, K.; Agasti, S. S.; Kim, C.; Li, X.; Rotello, V. M., Gold Nanoparticles in Chemical and Biological Sensing. *Chemical Reviews* **2012**, 112, 2739–2779.
- [5] Chinen, A. B.; Guan, C. M.; Ferrer, J. R.; Barnaby, S. N.; Merkel, T. J.; Mirkin, C. A., Nanoparticle Probes for the Detection of Cancer Biomarkers, Cells, and Tissues by Fluorescence. *Chemical Reviews* **2015**, 115, 10530-10574.
- [6] Liu, B.; Liu, J., Interface Driven Hybrid Materials Based on DNA-Functionalized Gold Nanoparticles. *Matter* **2019**, 1, 825-847.
- [7] Li, L. L.; Xing, H.; Zhang, J. J.; Lu, Y., Functional DNA Molecules Enable Selective and Stimuli-Responsive Nanoparticles for Biomedical Applications. *Accounts of Chemical Research* **2019**, 52, 2415-2426.
- [8] Liu, B., Salgado, S., Maheshwari, V., Liu, J., DNA Adsorbed on Graphene and Graphene Oxide: Fundamental Interactions, Desorption and Applications. *Current Opinion in Colloid & Interface Science* **2016**, 26, 41-49.
- [9] Mascini, M. Aptamers and Their Applications. *Analytical and Bioanalytical Chemistry* **2008**, 390, 987-988.
- [10] Huang, P. J. J., Liu, J., Selection of Aptamers for Sensing Caffeine and Discrimination of Its Three Single Demethylated Analogues. *Analytical Chemistry* **2022**, 94, 7, 3142–3149.
- [11] Huang, P. J. J., Liu, J., A DNA Aptamer for Theophylline with Ultrahigh Selectivity of the Classic RNA Aptamer. *ACS Chemical Biology* **2022**, 17, 8, 2121–2129.
- [12] OGAWA, N.; UEKI, H., Clinical Importance of Caffeine Dependence and Abuse. *Psychiatry and Clinical Neurosciences* **2007**, 61, 263-268.

- [13] Nakatsuka, N., Yang, K. A., Abendroth, J. M., Cheung, K. M., Andrews, A. M., Aptamer–Field-Effect Transistors Overcome Debye Length Limitations for Small-Molecule Sensing. *Science* **2018**, 362, 6412, 319-324.
- [14] Yang, K. A., Pei, R., Stojanovic, M. N., *In Vitro* Selection and Amplification Protocols for Isolation of Aptameric Sensors for Small Molecules. *Methods* **2016**, 106, 58-65.
- [15] Jenison, R. D.; Gill, S. C.; Pardi, A.; Polisky, B. High-Resolution Molecular Discrimination by RNA. *Science* **1994**, 263, 1425–1429.
- [16] Song, S., Wang, L., Li, J., Fan, C., Zhao, J., Aptamer-Based Biosensors. *TrAC Trends in Analytical Chemistry* **2018**, 27, 2, 108-177.
- [17] McConnell, E. M., Nguyen, J., Li, Y., Aptamer-Based Biosensors for Environmental Monitoring. *Frontiers in Chemistry* **2020**, 8, 434.
- [18] Zhou, W., Huang, P. J. J., Ding, J., Liu, J., Aptamer-Based Biosensors for Biomedical Diagnostics. *Analyst* **2014**, 139, 2627-2640.
- [19] Li, H.; Rothberg, L. J., Label-Free Colorimetric Detection of Specific Sequences in Genomic DNA Amplified by the Polymerase Chain Reaction. *Journal of American Chemical Society* **2004**, 126, 10958-10961.
- [20] Li, H.; Rothberg, L., Colorimetric Detection of DNA Sequences Based on Electrostatic Interactions with Unmodified Gold Nanoparticles. *Proceedings of the National Academy of Sciences of the United States of America* **2004**, 101, 14036-14039.
- [21] Zhang, F., Huang, P. J. J., Liu, J. Sensing Adenosine and ATP by Aptamers and Gold Nanoparticles: Opposite Trends of Color Change from Domination of Target Adsorption Instead of Aptamer Binding. *ACS Sensors* **2020**, 5, 9, 2885–2893.
- [22] Liu, B., Huang, Z., Ma, L., Liu, J., Bromide as a Robust Backfiller on Gold for Precise Control of DNA Conformation and High Stability of Spherical Nucleic Acids. *Journal of The American Chemical Society* **2018**, 140, 13, 4499-4502.
- [23] Song, K.-M.; Jeong, E.; Jeon, W.; Cho, M.; Ban, C., Aptasensor for Ampicillin Using Gold Nanoparticle Based Dual Fluorescence–Colorimetric Methods. *Analytical and Bioanalytical Chemistry* **2012**, 402, 2153-2161.
- [24] Zong, C.; Liu, J., The Arsenic-Binding Aptamer Cannot Bind Arsenic: Critical Evaluation of Aptamer Selection and Binding. *Analytical Chemistry*. **2019**, 91, 10887-10893.

- [25] Zong, C.; Zhang, Z.; Liu, B.; Liu, J., Adsorption of Arsenite on Gold Nanoparticles Studied with DNA Oligonucleotide Probes. *Langmuir* **2019**, 35, 7304-7311.
- [26] Zhou, J.; Li, Y.; Wang, W.; Lu, Z.; Han, H.; Liu, J., Kanamycin Adsorption on Gold Nanoparticles Dominates Its Label-Free Colorimetric Sensing with Its Aptamer. *Langmuir* **2020**, 36, 11490–11498.
- [27] Goldys, E. M., *Fluorescence Applications in Biotechnology and the Life Sciences*, 1; Wiley Blackwell, 2009.
- [28] Taraska, J. W., Zagotta, W. N., Fluorescence Applications in Molecular Neurobiology. *Neuron* **2010**, 66, 2, 170-189.
- [29] Zhong, W., Nanomaterials in Fluorescence-Based Biosensing. *Analytical and Bioanalytical Chemistry* **2009**, 394, 47-59.
- [30] Dong, H., Zhang, J., Ju, H., Lu, H., Wang, S., Jin, S., Hao, K., Du, H., Zhang, X., Highly Sensitive Multiple microRNA Detection Based on Fluorescence Quenching of Graphene Oxide and Isothermal Strand-Displacement Polymerase Reaction. *Analytical Chemistry* **2012**, 84, 10, 4587-4593.
- [31] Liu, Y., Liu, C. Y., Liu, Y., Investigation on Fluorescence Quenching of Dyes by Graphite Oxide and Graphene. *Applied Surface Science* **2011**, 257, 13, 5513-5518.
- [32] Chung, C., Kim, Y-K., Shin, D., Ryoo, S-R., Hong, B. H., Min, D-H., Biomedical Applications of Graphene and Graphene Oxide. *Accounts of Chemical Research* **2013**, 46, 10, 2211-2224.
- [33] Zhan, S., Yu, M., Lv, J., Wang, L., Zhou, P., Colorimetric Detection of Trace Arsenic(III) in Aqueous Solution Using Arsenic Aptamer and Gold Nanoparticles. *Australian Journal of Chemistry* **2014**, 67, 5, 813-818.
- [34] Liu, J., Cui, L., Losic, D., Graphene and Graphene Oxide as New Nanocarriers for Drug Delivery Applications. *Acta Biomaterialia* **2013**, 9, 12, 9243-9257.
- [35] Vieira, L. R.; Soares, A. M. V. M.; Freitas, R., Caffeine as a Contaminant of Concern: A Review on Concentrations and Impacts in Marine Coastal Systems. *Chemosphere* **2022**, 286, 131675.

- [36] Svorc, L., Determination of Caffeine: A Comprehensive Review on Electrochemical Methods. *International Journal of Electrochemical Science* **2013**, 8, 5755-5773.
- [37] González, N.; Lantmann Corral, S. P.; Zanini, G.; Montejano, H.; Acebal, C. C., An Inner Filter Effect Based Sensing System for the Determination of Caffeine in Beverage Samples. *Analyst* **2020**, 145, 2279-2285.
- [38] Xu, W.; Kim, T.-H.; Zhai, D.; Er, J. C.; Zhang, L.; Kale, A. A.; Agrawalla, B. K.; Cho, Y.-K.; Chang, Y.-T., Make Caffeine Visible: A Fluorescent Caffeine “Traffic Light” Detector. *Scientific Reports* **2013**, 3, 2255.
- [39] Journey, J. D., Bentley, T. P., *Theophylline Toxicity*; StatPearls Publishing, 2022.
- [40] Barnes, P. J., Theophylline. *Pharmaceuticals* **2010**, 3, 725-747.
- [41] Ozgun, D., Basak, S. & Cinar, O. The Inhibition Effect of Three Different Pharmaceuticals in Domestic Wastewater. *World Journal of Environmental Research* **2014**. 4(1), 01-06.
- [42] Feng, S.; Chen, C.; Wang, W.; Que, L., An Aptamer Nanopore-Enabled Microsensor for Detection of Theophylline. *Biosensors and Bioelectronics*. **2018**, 105, 36-41.
- [43] Jiang, H.; Ling, K.; Tao, X.; Zhang, Q., Theophylline Detection in Serum Using a Self-Assembling RNA Aptamer-Based Gold Nanoparticle Sensor. *Biosensors and Bioelectronics*. **2015**, 70, 299-303.
- [44] Chávez, J. L., Lyon, W., Kelley-Loughane, N., Stone, M. O., Theophylline Detections Using an Aptamer and DNA-Gold Nanoparticles Conjugates. *Biosensors and Bioelectronics* **2010**, 26, 1, 23-28.
- [45] Tao, X., Peng, Y., Liu, J., Nanomaterial-Based Fluorescent Biosensors for Veterinary Drug Detection in Foods. *Journal of Food and Drug Analysis* **2020**, 28, 4, 575-594.
- [46] Nguyen, D-K., Jang, C-H., A Simple and Ultrasensitive Colorimetric Biosensor for Anatoxin-a Based on Aptamer and Gold Nanoparticles. *Micromachines* **2021**, 12, 12, 1526.
- [47] Zahra, Q. U. A., Luo, Z., Ali, R., Khan, M. I., Li, F., Qiu, B., Advances in Gold Nanoparticles-Based Colorimetric Aptasensors for the Detection of Antibiotics: An Overview of the Past Decade. *Nanomaterials* **2021**, 11, 4, 840.

- [48] Ma, X., Guo, Z., Mao, Z., Tang, Y., Miao, P., Colorimetric Theophylline Aggregation Assay Using an RNA Aptamer and Non-Crosslinking Gold Nanoparticles. *Mikrochimica Acta* **2017**, 185, 1, 33.
- [49] Katiyar, N., Selvakumar, L. S., Patra, S., Thakur, M. S., Gold nanoparticles based colorimetric aptasensor for theophylline. *Analytical Methods* **2013**, 5, 653-659.
- [50] Zhang, F., Liu, J., Label-Free Colorimetric Biosensors Based on Aptamers and Gold Nanoparticles: A Critical Review. *Analysis & Sensing* **2020**, 1, 1, 30-43.
- [51] Liu, X., Zhang, F., Zhang, Z., Huang, Z., Liu, J., Dopamine and Melamine Binding to Gold Nanoparticles Dominates Their Aptamer-Based Label-Free Colorimetric Sensing. *Analytical Chemistry* **2020**, 92, 13, 9370-9378.
- [52] Hu, Y., Huang, Z., Liu, B., Liu, J., Hg(II) Adsorption on Gold Nanoparticles Dominates DNA-Based Label-Free Colorimetric Sensing. *ACS Applied Nano Materials* **2021**, 4, 2, 1377-1384.
- [53] Pavel, I., Szeghalmi, A., Moigno, D., Cîntă, S., Kiefer, W., Theoretical and pH Dependent Surface Enhanced Raman Spectroscopy Study on Caffeine. *Biopolymers* **2002**, 71, 1, 25-37.
- [54] Liu, P., Liu, R., Guan, G., Jiang, C., Wang, S., Zhang, Z., Surface-Enhanced Raman Scattering Sensor for Theophylline Determination by Molecular Imprinting on Silver Nanoparticles. *Analyst* **2011**, 136, 4152-4158.
- [55] Muniz-Miranda, F., Pedone, A., Muniz-Miranda, M., Raman and Computational Study on the Adsorption of Xanthine on Silver Nanocolloids. *ACS Omega* **2018**, 3, 10, 13530-13537.
- [56] Cavalieri, L., F., Fox, J. J., Stone, A., Chang, N., On the Nature of Xanthine and Substituted Xanthines in Solution. *Journal of the American Chemical Society* **1954**, 76, 4, 1119-1122.
- [57] Liu, J., Lu, Y., Preparation of Aptamer-Linked Gold Nanoparticle Purple Aggregates for Colorimetric Sensing of Analytes. *Nature Protocols* **2006**, 1, 246-252.
- [58] Aldrich, M. B., Blackburn, M. R., Kellems, R. E., The Importance of Adenosine Deaminase for Lymphocyte Development and Function. *Biochemical and Biophysical Research Communications* **2000**, 272, 2, 311-315.

[59] Fredholm, B. B., Adenosine, Adenosine Receptors and the Actions of Caffeine. *Pharmacology & Toxicology* **1995**, 76, 2, 93-101.

[60] Lu, C-H., Lin, M-H., Wang, Y-W., Yang, H-H., Chen, X., Chen, G-N., Amplified Aptamer-Based Assay through Catalytic Recycling of the Analyte. *Angewandte Chemie* **2010**.

[61] Hideshima, S., Sato, R., Inoue, S., Kuroiwa, S., Osaka, T., Detection of Tumor Marker in Blood Serum Using Antibody-Modified Field Effect Transistor with Optimized BSA Blocking. *Sensors and Actuators B: Chemical* **2012**, 161, 1, 146-150.

[62] Jeyachandran, Y. L., Mielczarski, J. A., Mielczarski, E., Rai, B., Efficiency of Blocking of Non-Specific Interaction of Different Proteins by BSA Adsorbed on Hydrophobic and Hydrophilic Surfaces. *Journal of Colloid Interface Science* **2010**, 341, 136-142.